Research on cold forming of tubular electrode plates for lead-acid batteries

Diploma Thesis

by

Zhai Hui

durchgeführt am

Lehrstuhls für Umformtechnik, Department Product

Engineering

an der Montanuniversität Leoben, Austria

Leoben, March 2010

Declaration of originality

I hereby declare that I composed this thesis by myself without any assistance from third parties. Furthermore, I confirm that on sources and resources have been used in the preparation of this thesis other than those indicated in the thesis itself. All references have been cited as appropriate.

Leoben, March, 2010   ZHAI HUI

Acknowledgements

First of all, I would like to extend my sincere gratitude to my advisor, Professor Bruno Buchmayr, for his instructive advice and the useful suggestions on my thesis. I am deeply grateful for his help in the completion of this thesis.

I want to express my gratitude towards Ing.Christian Arzt of BM-Battery Machines GmbH for the excellent cooperation. He offered me professional information concerning batteries and much technical support.

Also I wish to thank Dr.Thomas Hatzenbichler, Mr. Christian Stöckl and Mr. Ralph Ambrosch of Chair of Metal Forming, Leoben, for their selfless help during the writing of my thesis.

Last my thanks would go to my beloved family for their loving considerations and great confidence in me all through these years. I also owe my sincere gratitude to my friends and my fellow classmates who gave me their help and time in listening to me and helping me work out my problems during the difficult course of the thesis.

Abstract

The traditional manufacturing method of a lead batteries tubular plate is casting. To improve the tubular plate quality, to reduce production cost, to protect environment and human health in production a new manufacturing method is needed. The task of this thesis is to analyse the feasibility of using cold extrusion by laboratory tests and application trials.

A series of compression tests were performed to measure flow stress of lead and lead-antimony alloy (Sb 3.5%) at different temperatures. According to the test results, cold extrusion dies were designed. On the basis of products quality analysis and laboratory tests using cold extrusion, the manufacturing processes die-casting and cold extrusion were compared and evaluated. Based on our study, cold extrusion is proved to be suitable for production of battery tubular plate. Further suggestions of modification of production process using cold extrusion are presented.

Kurzfassung

Üblicherweise werden Polplatten für Bleibatterien gegossen, jedoch werden aufgund des Umwelt- und Arbeitsschutzes und zur Senkung des Herstellkosten alterative Herstellverfahen gesucht. Als mögliche Herstellvariante wird in dieser Anteil das Kaltfließpressen betrachtet. Dazu wurde mit Reinblei und PbSb (3.5%)-Legierung Fließkurven bei unterschiedliche Temperatur aufgenommen. Weiters wurden vereinfachte Fließpresswerkzeuge gebaut und Extrusionsversuche durchgeführt. Die Auswertungen und die Verfahrensvergleiche haben gezeigt, daß die Polplatte prinzipiell mit Kaltfließpressen herstellbar ist. Im Ausblick werden auch Hinweise zur Verbesserung des Fertigungprozesses angegeben.

Schlagwörter: Batterie Polplatte ; Blei und Bleilegierungen; Kaltumformung; Fließpressen

List of symbols and abbreviations

Computation Abb.	Explanations
A	Area, $[\text{mm}^2]$
A_0	Cross sectional area of the container, $[\text{mm}^2]$
A_1	Cross sectional area of the extruded product, $[\text{mm}^2]$
d	Billet diameter, $[\text{mm}]$
d_0	Stem (dummy block) diameter, $[\text{mm}]$
d_1	Inside diameter of die, $[\text{mm}]$
D_0	Container diameter, $[\text{mm}]$
F	Load (compression, tensile, torsion) , $[\text{N}]$
F_{id}	Ideal extrusion load, $[\text{N}]$
F_F	Frictional load, $[\text{N}]$
F_T	Total (extrusion) load, $[\text{N}]$
h_0	Depth of container, $[\text{mm}]$
h_1	Depth of the die, $[\text{mm}]$
h_2	Length of the die land, $[\text{mm}]$
k_w	Deformation resistance, $[\text{N/mm}^2]$
k_f	Flow stress, $[\text{N/mm}^2]$
K_m	Mean deformation resistance, $[\text{N/mm}^2]$
L	Instantaneous billet length, $[\text{mm}]$
n	Number of the die land, $[-]$

R_m	Tensile strength, [N/mm^2]
T	Temperature, [°C]
T_M	Melting point, [°C]
U	Circumference, [mm]
φ	Logarithmic strain, [-]
$\dot{\varphi}$	Strain rate, [S^{-1}]
φ_{Fr}	Strain to fracture, [-]
η_F	Deformation efficiency factor, [-]
μ	Friction coefficient, [-]

Contents

1 Introduction

Due to intense global competition, the battery industry is also confronted with very short product life cycles and continually rising requirements on the product quality.

It is general knowledge that battery electrodes are the most important component of lead acid batteries and have a direct effect on the lifetime of a battery. The main components of electrodes are lead and lead alloy, a poisonous metal. Due to rising costs and environmental protection pressures, the requirements for the manufacturing process of the perfect battery and its components are growing. Manufactures require productive and accepted methods to face these challenges, which can be provided by suitable modern forming processes.

1.1 Motivation and goal of this thesis

The traditional manufacturing process of the electrode plate is die-casting. Although die-casting has many advantages, the quality of products should be increase. In addition, improving the working conditions by reducing the harmful metal vapors which are emitted during the die-casting process detrimental to health and environment is very important.

The forming process is feasible as a solution to these problems. Cold forming is prevalent and a relatively simple process for the deformation of metal. Cold extrusion is one of the most important metals forming processes of metals due to its high productivity, lower costs and improvement of the physical properties of metals.

Fundamental consideration of the raw material of a tubular plate leads to the requirement of a soft heavy metal. The forming of lead and its alloys at room

temperature is a possibility for manufacturing, as the physical properties and deformation ability make it easy to extrude.

The task of this thesis is to discuss the feasibility of using cold extrusion and suggest a more detailed plan for application. A series of forming tests were performed to measure stress flow at different temperatures and the change in microstructure. Cold extrusion models were designed according to the results of prior tests. The quality of the product is investigated after cold extrusion. The manufacturing processes die-casting and cold extrusion will be compared and evaluated.

The master thesis was performed in close cooperation with BM-Battery Machines GmbH in Ebersdorf near Hartberg.

1.2 Structure of this thesis

The following structure was chosen to present this thesis: Chapter 2 offers an explanation of the fundamentals of batteries and the battery industry. The types of batteries available, chemical reactions and the components of batteries are illustrated. The differences between the tubular plate and flat plate are explained as well. The standard manufacturing method of tubular plates is introduced in chapter 3 and the new method along with its advantages and disadvantages are discussed as well.

Lead is necessary raw material for producing battery electrodes. The properties of pure lead and its alloys are considered in chapter 4. A short description of the deformation ability and extrusion character of lead and its alloys are illustrated.

The main part of this thesis, performing a series of experiments to observe the forming properties of lead and its alloys, is presented in chapter 5. The flow stresses of raw materials resulting from the compression experiments will be applied to the

following cold extrusion tests. In addition, two specialized extrusion models will be designed: one to extrude single lead spines and the other to extrude a whole small tubular plate in the laboratory. Following the experiments, the internal microstructures of specimens or work pieces will be observed. Through a discussion and analysis of the results of the tests, a general conclusion as to the feasibility of the extrusion of a lead tubular plate at room temperature concludes chapter 5.

In chapter 6, the different manufacturing possibilities of a tubular plate will be compared and advantages and disadvantages discussed. Moreover, a process layout for industrial production will be recommended. The final conclusion and future prospects can also be found in chapter 6.

Finally, the references used and refered to are listed in chapter 7.

2 Fundamentals of the lead-acid battery

2.1 Introduction of the lead-acid battery

Lead-acid batteries, invented in 1859 by the French physicist Gaston Planté, are the oldest type of rechargeable battery. Despite having the second lowest energy-to-weight ratio (next to the nickel-iron battery) and a correspondingly low energy-to-volume ratio, their ability to supply high surge currents means that the cells maintain a relatively large power-to-weight ratio. These features, along with their low cost, make them attractive for use in motor vehicles [1].

A car battery is a type of rechargeable battery that supplies electric energy to the starter motor in an automobile. The battery is also referred to as an SLI battery (starting, lighting and ignition) to power the starter motor, the lights, and the ignition system of a vehicle's engine. This also may describe a traction battery used for the main power source of an electric vehicle. Automotive starter batteries (lead-acid type) provide a nominal 12-volt potential difference by connecting six galvanic cells in series. Each cell provides 2.1 volts for a total of 12.6 volt at full charge [1].

Energy/weight:	30~40 Wh/kg
Energy/size:	60~75 Wh/L
Power/weight:	180 W/kg
Charge/discharge efficiency:	50%-92%
Self-discharge rate:	3%-20%/ month
Cycle durability:	500-800 cycles
Nominal Cell Voltage	2.105 V

Figure 1: The parameter of an automotive starter battery [2].

2.2 Types of lead-acid batteries and their structure

A lead-acid battery consists of an electrode comprising of lead and lead oxide and an electrolyte comprising of sulfuric acid. There are many different sizes and designs of lead-acid batteries, but the most important designation is whether they are deep cycle batteries or shallow cycle batteries [3].

Shallow cycle batteries, like the type used as a starting battery in automobiles, are designed to supply a large amount of current for a short time and withstand mild overcharge without losing electrolyte. However, they cannot tolerate being deeply discharged. In fact, the lifetime of a shallow cycle battery is considerably shortened if they are repeatedly discharged by more than 20 percent.

 Deep cycle batteries, on the other hand, are designed to be discharged repeatedly by as much as 80 percent of their capacity. This characteristic explains their use in power systems. Although they are designed to withstand deep cycling, the lifetime of deep cycle batteries is longer if the cycles are shallower. All lead-acid batteries will fail prematurely if they are not recharged completely following each cycle. Letting a lead-acid battery stay in a discharged condition for many days at a time will cause sulfating of the positive plate and a permanent loss of capacity.

Sealed deep-cycle lead-acid batteries are maintenance free. They never need watering or an equalization charge. They cannot freeze or spill, so they can be mounted in any position. Sealed batteries require very accurate regulation to prevent overcharge and over discharge. Either of these conditions will drastically shorten their lives. Sealed batteries are therefore well-suited for remote, unattended power systems.

Details of the design, metal contents, capacities, etc. of lead-acid storage batteries can be found in the new German Standard Specifications DIN 40730 to 40737.

Lead storage batteries are classified according to their use as follows [4]:

1. Traction batteries for use in driving vehicles or in power plants
2. Lighting batteries for train lighting or emergency lighting for instance
3. Batteries for communication purposes, e.g. for telephone systems
4. Batteries for auxiliary services, e.g. for control and recording systems, braking systems
5. Start batteries for the ignition of automobiles as well as for lighting

The most important elements of lead-acid battery are battery plates and separators. The principle of the lead acid cell can be demonstrated with simple sheet lead plates for the two electrodes. Each plate consists of a rectangular lead grid alloyed with antimony or calcium to improve the mechanical characteristics. The holes of the grid are filled with a mixture of red lead and 33% dilute sulfuric acid. (Different manufacturers have modified the mixture). The paste is pressed into the holes in the plates which are slightly tapered on both sides to assist in retention of the paste. This porous paste allows the acid to react with the lead inside the plate, increasing the surface area manifold. At this stage the positive and negative plates are similar; however expanders and additives vary their internal chemistry to assist in operation when in use. Once dry, the plates are then stacked together with suitable separators and inserted in the battery container. After the acid has been added to the cell, the cell is given its first forming charge. The positive plates gradually turn the chocolate brown color of lead dioxide, and the negative turn the slate gray of 'spongy' lead [31]. The cell is ready to be used after formation.

Separators are used between the positive and negative plates of a lead acid battery to prevent short circuit through physical contact, mostly through dendrites ('treeing'), but also through shedding of the active material. Separators obstruct the flow of ions between the plates and increase the internal resistance of the cell. Various materials have been used to make separators, including wood, rubber, glass fiber mat, cellulose, and PVC or polyethylene plastic.

Figure 2 shows the structure of a normal lead acid battery. A 12V lead-acid battery is made up of six cells, each cell producing approximately 2.11V. The cells are connected in series from positive terminal of the first cell to the negative terminal of the second cell and so on. Each cell is made up of an element containing positive plates and negative plates and the cells are also connected together. The individual cells are separated by thin sheets of electrically insulated porous material called „envelopes" or "separators". They isolate the positive and negative plates to keep them from electrically shorting one other.
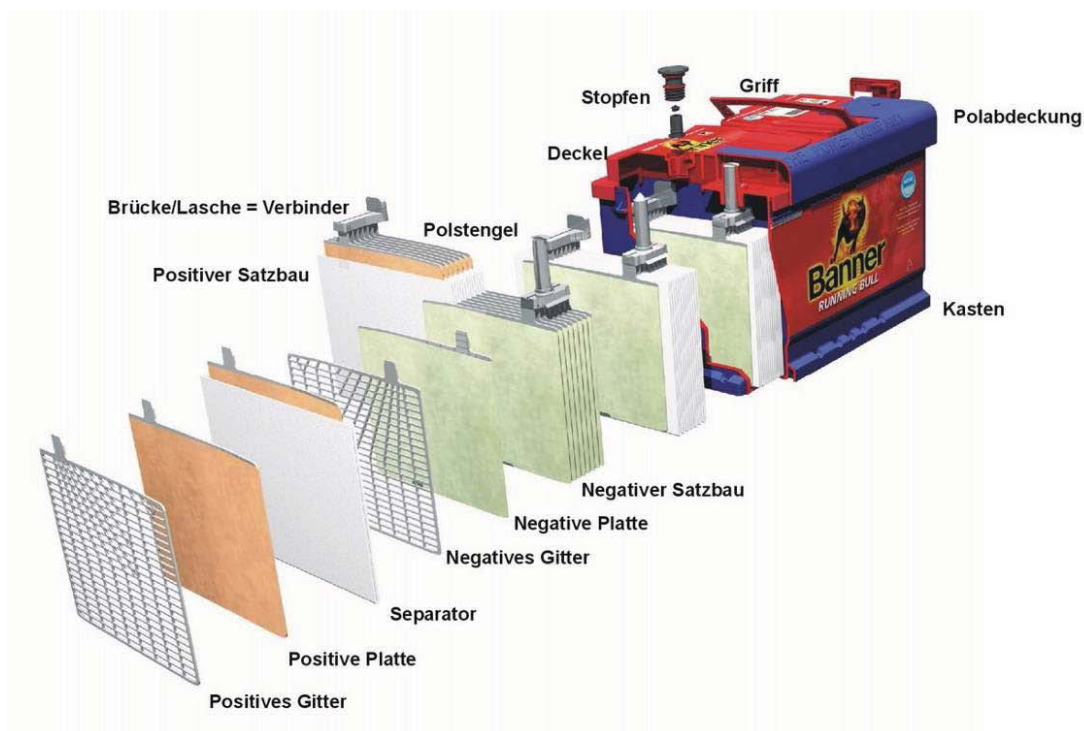
Figure 2: The structure of a car battery [5]

2.3 Electrochemistry of a lead-acid battery

Lead-acid batteries are made up of lead plates and lead oxide plates, which are submerged in an electrolyte solution of about 35% sulfuric acid and 65% water [1]. This causes a chemical reaction that releases electrons, allowing them to flow through conductors to produce electricity. As the battery discharges, the acid of the electrolyte reacts with the plate materials, changing their surfaces to lead sulfate. When the battery is recharged, the chemical reaction is reversed: the lead sulfate regresses into lead oxide and lead respectively. With the plates restored to their original condition, the process may now be repeated.

Figure 3a and Figure 3b show the charging and discharging process of a lead-acid battery respectively. Because most lead-acid batteries have open cells with liquid electrolyte, overcharging with excessive charging voltages will generate oxygen and hydrogen gas by electrolysis of water, forming an explosive mix. The acidic electrolyte is also corrosive. In practice, cells are usually not made of pure lead but contain small amounts of antimony, tin, calcium or selenium alloyed in the plate material.
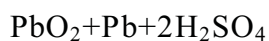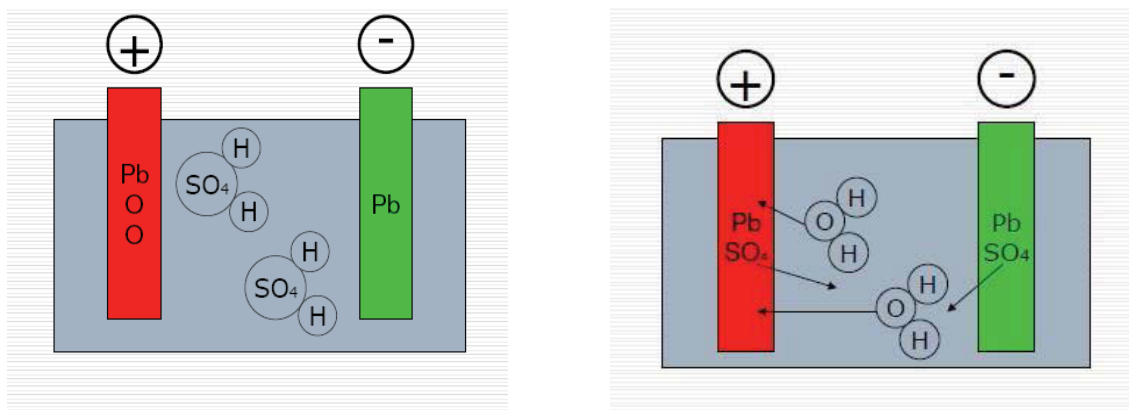
$PbO_2 + Pb + 2H_2SO_4$ Acidity increased

Acidity level ~1,28

Figure 3 a: Charging process of a lead-acid battery [5]
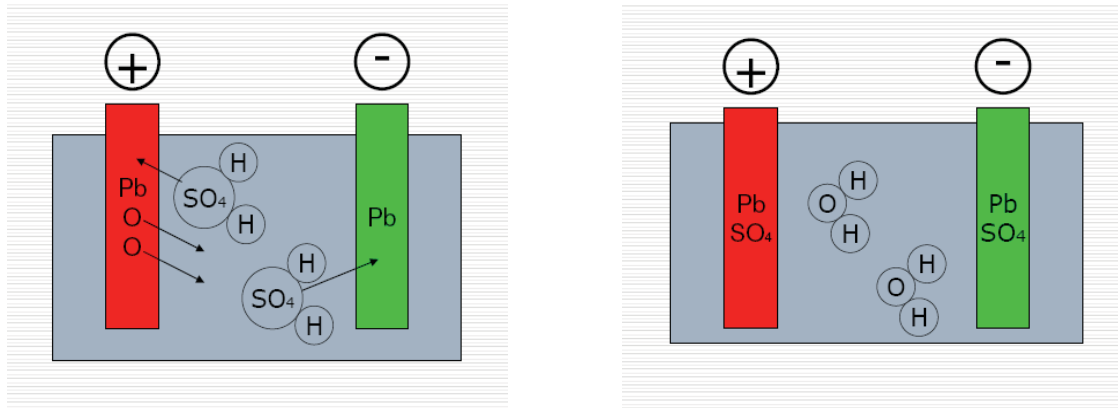
Acidity decreased $PbSO_4+PbSO_4+2H_2O$

water

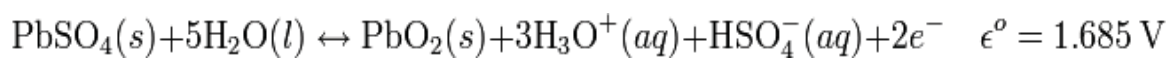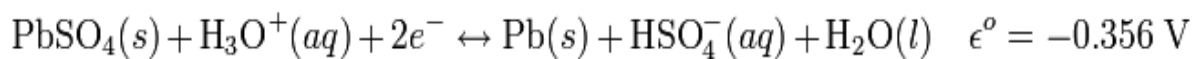Figure 3 b: Discharging process of a lead-acid battery [5]

The chemical reactions at the electrode are written as follows [6]:

At the cathode (Reduction):

$$PbSO_4(s)+5H_2O(l) \leftrightarrow PbO_2(s)+3H_3O^+(aq)+HSO_4^-(aq)+2e^- \quad \epsilon^o = 1.685 \text{ V}$$

At the anode (Oxidation):

$$PbSO_4(s)+H_3O^+(aq)+2e^- \leftrightarrow Pb(s)+HSO_4^-(aq)+H_2O(l) \quad \epsilon^o = -0.356 \text{ V}$$

2.4 Assembly of a lead-acid battery

Battery assembly combines the plates, container, and other parts into a functional battery. Battery charging is also an important part of assembly. Figure 4 shows the assembly of a battery in detail [7].

The main assembly processes are:

➢ Stacking

After curing, the plates are stacked either by hand or by machine so that positive and negative plates alternate with an insulating separator in between.

➢ Group Burning

After the plates have been stacked, they are joined with small connecting parts and burned together to form cell elements or groups. This operation is conducted either manually at a burning station or by using an automatic cast-on-strap (COS) machine.

➢ Intercell Welding and Post Burning

After workers place all the groups in the battery case, the straps are fused together using a torch or high voltage electrical power source. This process can also be accomplished Through the Partition (TTP), using a case that has been punched. The connections are then welded. The units are tested and the posts are attached. The major source of lead exposure comes from lead fumes during the inter-cell welding process.

➢ Formation

In the dry charge (plate) formation process, the first step, called tacking consists of plates being placed in a tank and lead bars being welded, or "tacked" on. Battery plates are then formed (or charged) in tanks. The major source of lead exposure in

the formation process comes from lead fumes. Wet (case) formation is not associated with lead exposure during formation because the batteries are assembled and filled with acid prior to charging.
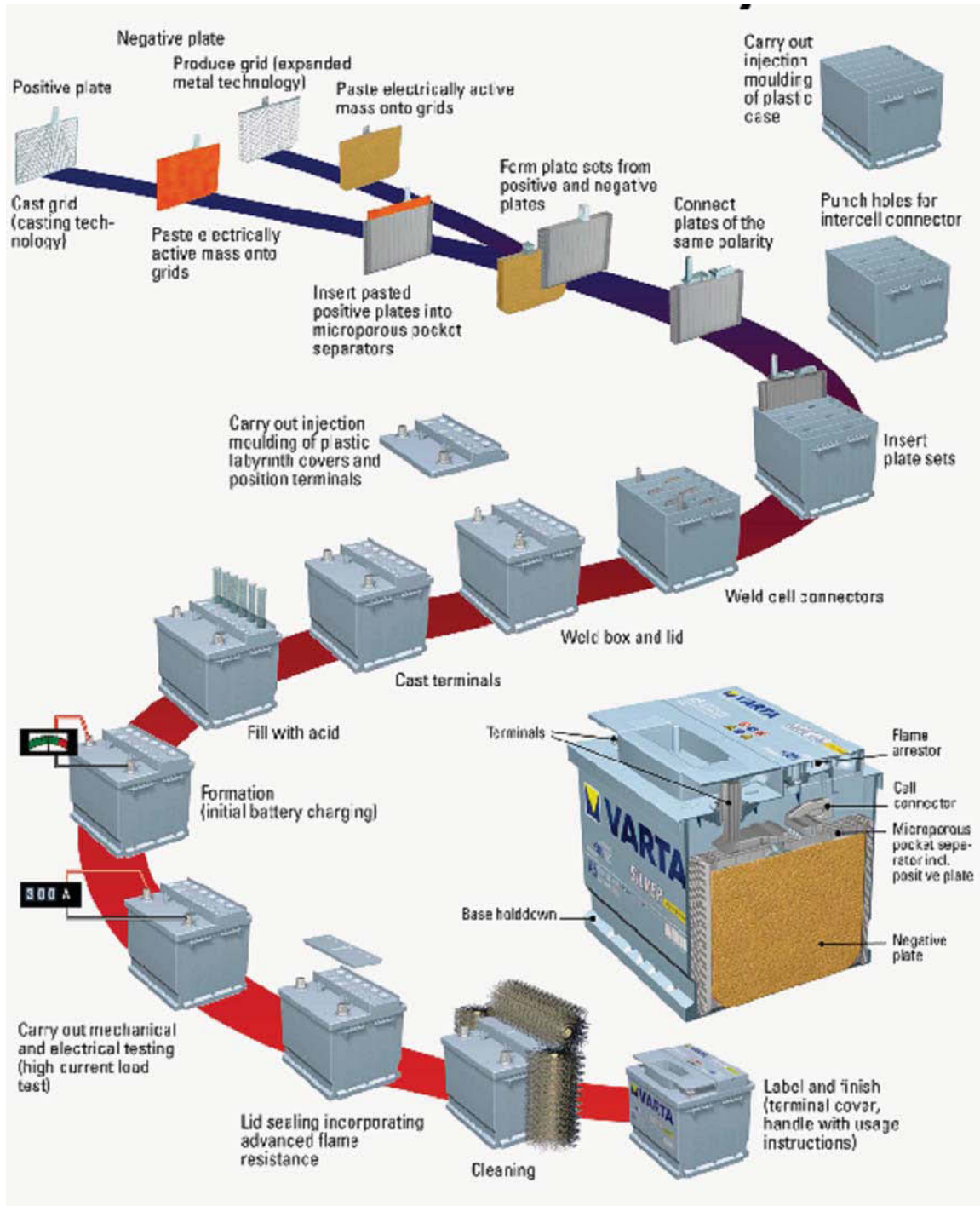

Figure 4: Assembly of a lead-acid battery [8]

3 Manufacturing of lead-acid battery tubular plates

3.1 Comparison of two types of the lead-acid battery plates

Flat plates and tubular plates are two basic types of store batteries available to the user today. These two battery plate types get their name from the design of the positive plate, as the negative plates are generally identical for both types. The essential difference in the flat plate design is that the positive plate is a rugged lead alloy grid filled with a specially compounded paste active material whereas in the tubular design, the positive plate is composed of a series of parallel tubes filled with lead oxide [9].
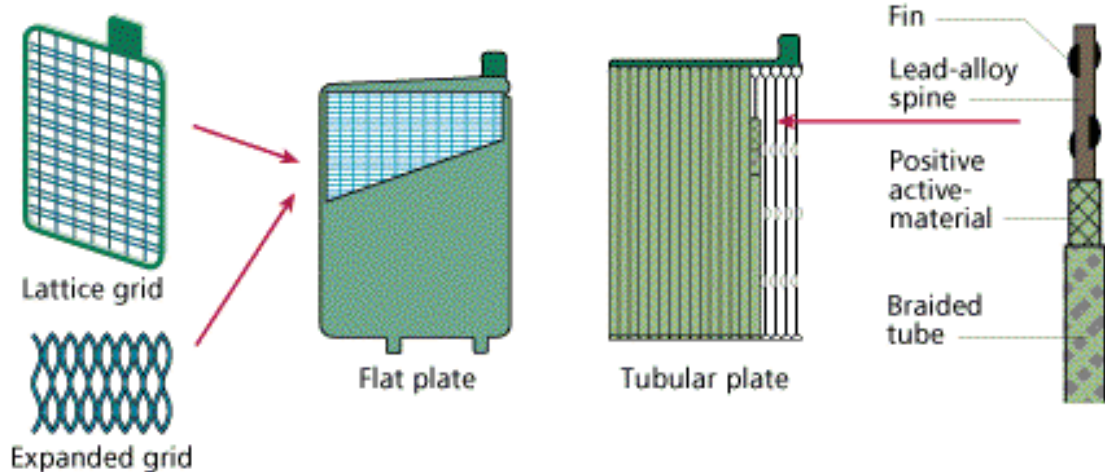

Figure 5: The two types of battery plates.

The picture on the left shows a normal flat plate whereas the picture on the right shows a tubular plate containing spines with fins [10].

The characteristics of batteries with flat plates [9]

> ➢ Good electrical performance
> ➢ Long lifecycle
> ➢ Durable
> ➢ Adequate reserves of pasted material for long life
> ➢ Adequate reserves of lead for long life
> ➢ Glass wrap protects the plate against life limiting shedding

The characteristics of batteries with tubular plates [9]

> ➢ Good electrical performance
> ➢ Adequate life
> ➢ Low reserves of lead
> ➢ Low reserves of active material
> ➢ Sensitive to active material shedding, which shortens cell life
> ➢ Sensitive to top bar breakage leading to a significant loss of plate area
> ➢ Sensitive to spines being off center in the tube leading to a significant loss of plate capacity

This thesis will concentrate on the tubular plate manufacturing process only.

3.2 Structure of the tubular plate of a lead-acid battery

The manufacturing process begins with the production of the grid which is typically a series of fifteen parallel lead rods or spines cast on to a bar. The grid structure in tubular plate batteries is made from a lead alloy. A pure lead grid structure is not strong enough by itself to stand vertically while supporting the active material. Other metals in small quantities are alloyed with lead for added strength and improved electrical properties. The most commonly alloyed metals are antimony, tin and calcium [2].

Top bar with lug

Carrots

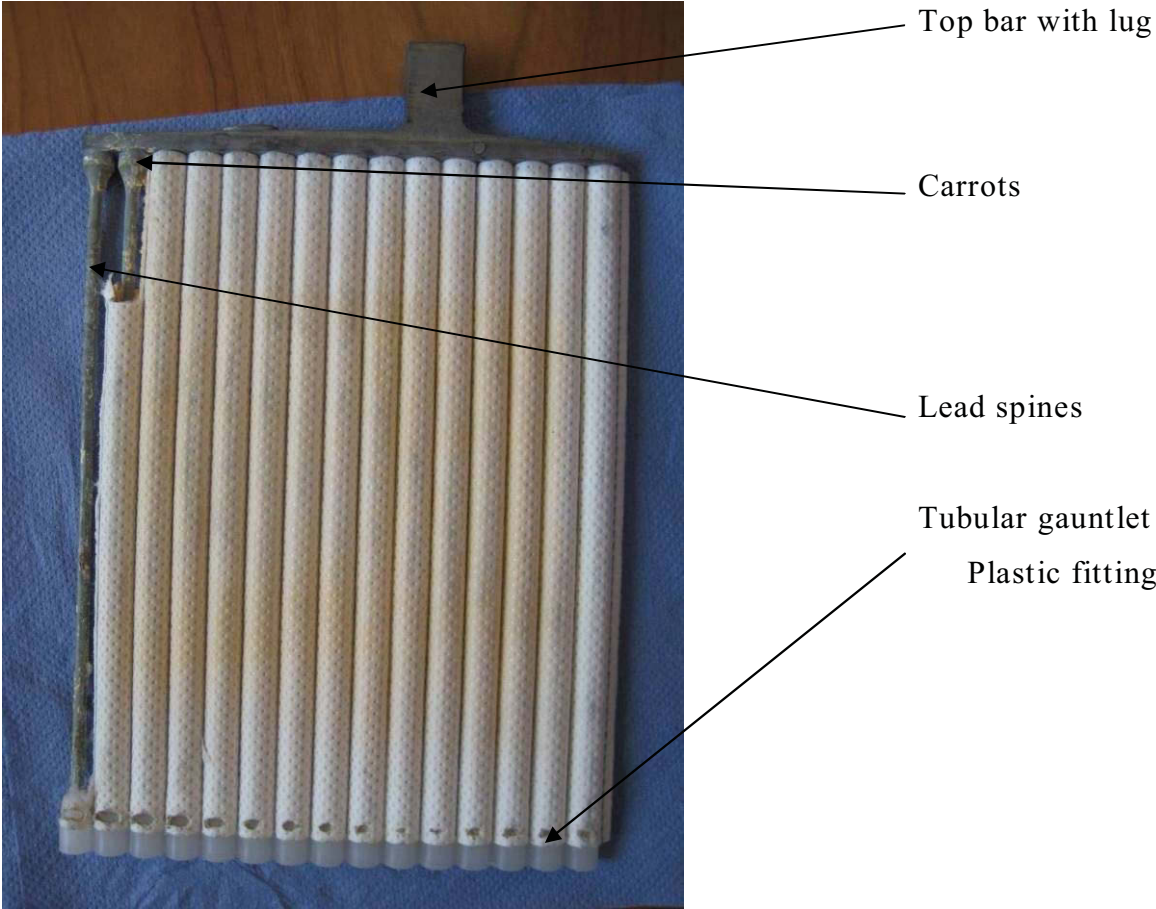Lead spines

Tubular gauntlet
Plastic fitting

Figure 6: The tubular plate of lead-acid battery [5].

Figure 6 is a photo from a tubular plate. Following the casting process of the main body, a series of parallel porous glass fiber tubes are fitted over the grid spines. These tubes are then filled with a mixture of lead oxide and red lead powder by vibration. Once the tubes are filled, they are sealed at the end of the lead grid spines by a plastic fitting. The resulting assembly is then soaked in diluted sulfuric acid to convert the lead oxide into lead sulfate. The finished product comprises a series of tubes filled with lead sulfate and a center core of lead to carry the current.

3.3 Casting of the tubular plate and its challenges

The traditional manufacturing method of a battery's tubular plate is casting. In the following section, various casting methods will be presented. The disadvantages of the standard die casting method commonly used in battery plate manufacturing will be introduced first.

3.3.1 Introduction to casting methods

Castings are used to form metals in their liquid form, moldable plastics or various other materials. Casting is most often used for producing complex shapes that would otherwise be difficult or uneconomical to manufacture using other production methods.

Metal castings can be classified into two types: expendable mold casting and non-expendable mold casting. Expendable mould casting is a generic classification including moldings made of sand, plastic, shell, plaster, and investment moldings (lost-wax technique). Non-expendable mold casting differs from expendable processes in that the mold need not be reformed after each production cycle. This technique includes at least four different methods: permanent, die, centrifugal and

continuous casting. Some of the major casting techniques involved in the commercial foundry is sand casting, die-casting, and investment casting [11].

The introduction and comparison of different casting methods follow:

Sand Casting:

Sand casting is one of the most popular and simplest types of casting and has been used for centuries. A sand casting or a sand molded casting is a cast part produced by forming a mould from a sand mixture and then pouring molten liquid metal into the cavity of the mould. The mould is then cooled until the metal has solidified. In the last stage, the casting is separated from the mould.

Sand casting allows for the production of smaller quantities at a reasonable cost compared to permanent mould casting. Not only does this method allow manufacturers to manufacture products at a low cost, but also small component sizes are possible. Depending on the type of sand used for the moulds, sand casting allows for most metals to be cast. Compared to other casting processes, the dimensional accuracy and surface quality are inferior and larger tolerances are required [12].

Investment Casting:

Investment casting derives its name from the fact that the pattern is invested or surrounded by a refractory material. The wax patterns require extreme care for they are not strong enough to withstand the forces encountered during the mold making. One advantage of investment casting is that wax can be reused.

The process is suitable for the repeated production of net shape components from a variety of different metals and high performance alloys. It can be an expensive process compared to other casting processes such as die-casting or sand casting, however the components that can be produced using investment casting can

incorporate intricate contours and, in most cases, the components are cast near net shape, so they require little or no rework after casting[12].

Die Casting:

The die-casting process forces molten metal into mould cavities under high pressure. Most die-castings are made from nonferrous metals, specifically zinc, copper, lead and aluminum based alloys, but ferrous metal die-castings are also possible. The die-casting method is especially suited for applications in which many small to medium sized parts are needed with highly detailed contours and fine surface quality as well as dimensional consistency.

Die-casting is a versatile process enabling the high-speed production of complex and intricate applications on a mass scale. Die-casting has simplified assembly line production in the engine and metal industries and has enabled the production of durable products.

3.3.2 Die-casting of the tubular plate and possible defects

The tubular plate is produced almost exclusively by die-casting and the battery plates are cast by top pouring. For large quantities, for instance grids for starter batteries, machines are used for casting and cutting mechanically. At each operation, molten metal delivered by a pump runs into the mould form, a heated casting trough above and parallel to the ingate. Figure 7 shows the casting of battery plates. According to type and alloy, the mould temperature is between 180°C and 220°C. Before each cast, the moulds are dusted with cork powder, water glass suspension DROTSCHMANN [13].

Manufacturing the battery plate with die-casting method has obviously many advantages, for example:

➢   It is a relatively low cost and easy method to produce battery plate,

➢   Die casting provides complex shapes within closer tolerances,

➢   Little or no machining is required after casting,

➢   No material is wasted,
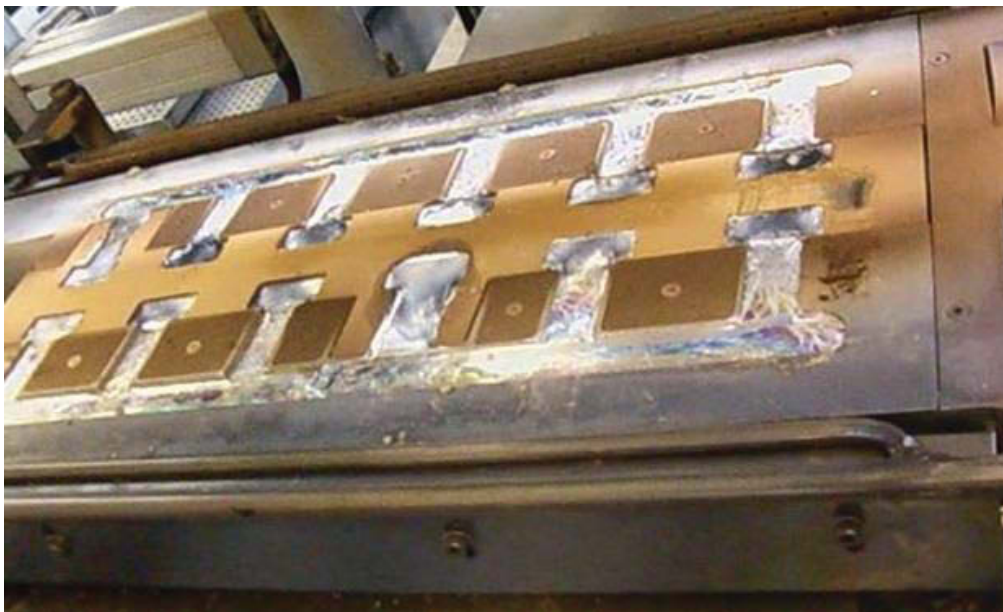
➢   Good dimensional accuracy…

Figure 7: The casting of battery plates [5]

However, there are also many disadvantages. Besides the expensive initial costs of die-casting, a large amount of energy is required to melt the casting materials. Furthermore, lead is a poisonous heavy metal and the vapour released during the casting process is hazardous to the environment and health of people. The biggest disadvantage is the appearance of certain defects in cast parts, which can not be avoided when casting. The following is a summary of the defects caused during casting.

➢ Surface defects of lead spines

As seen in figure 8, cracks appear on the surface of castings due to the surface tension after cooling. In addition, the flow marks are easily produced. In contrast to surface cracks, the flow marks appear as lines tracing the flow of liquid metal.
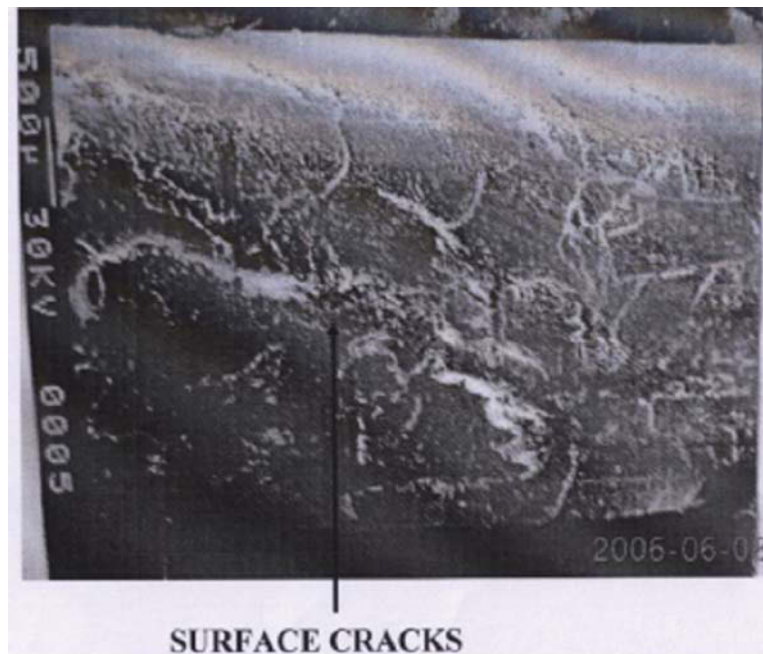

Figure 8: Surface cracks on lead spines [5]

➢ Internal defects of lead spines

Many defects can appear within the spine when the die-casting method is used, for example gas porosity, internal cracks, shrinkage defects and inclusions. Figure 9 and 10 show cracks and porosities found in die-casted spines.
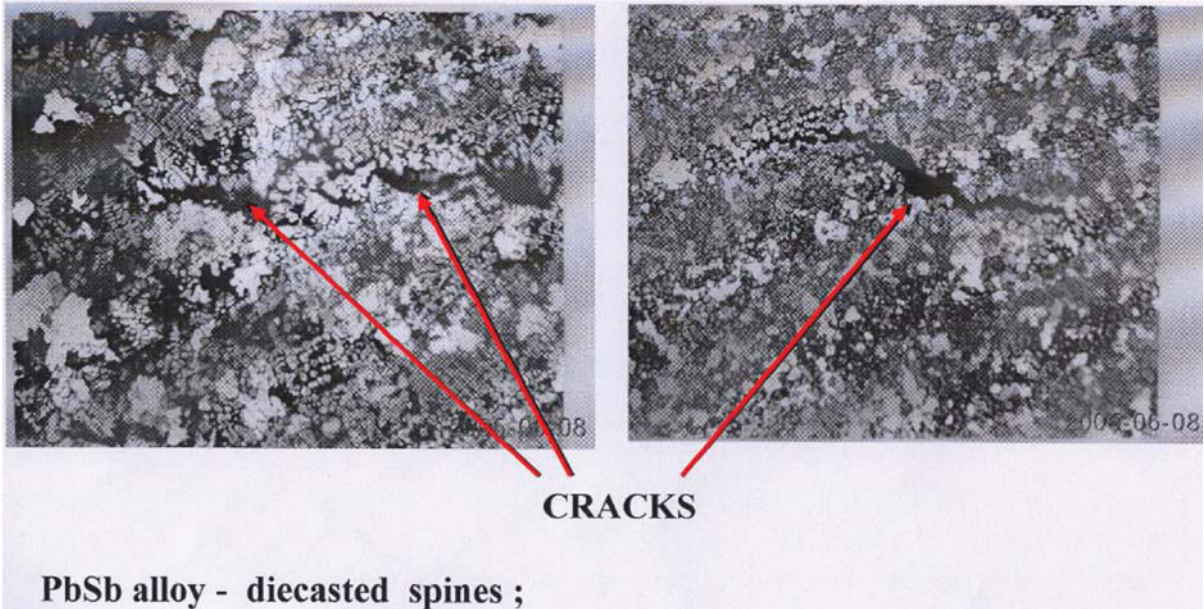
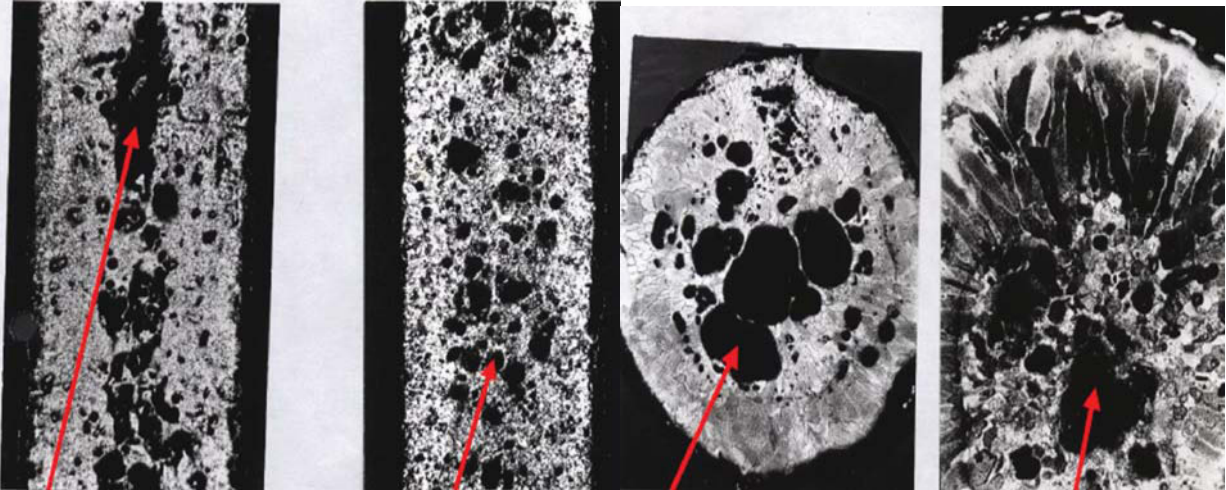Figure 9: Cracks in the lead-antimony die-casted spines [5]

Figure 10 a: Porosities in a longitudinal   Figure 10 b: Porosities in a cross section of
section of a lead spine [5]   a lead spine [5]

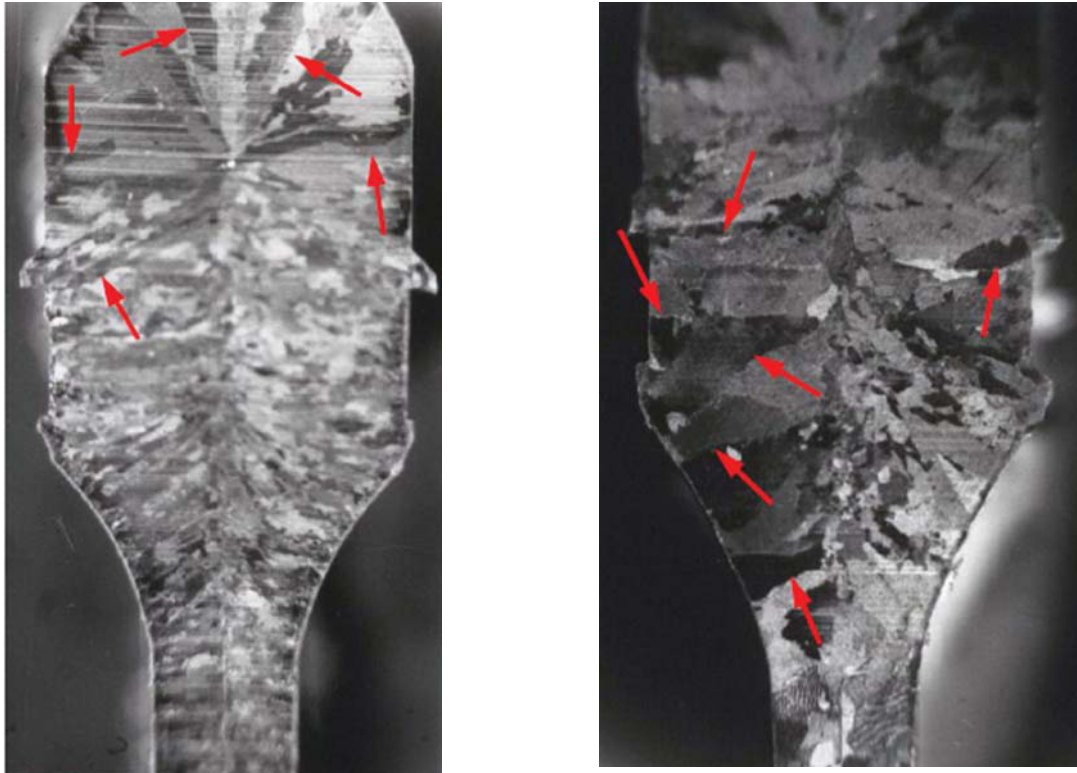The porosities pictured above were most likely due to gases or shrinkage.

Figure 11: Longitudinal section of a lead spine [5]

Figure 11 shows two pictures of the longitudinal section of a lead-antimony spine [5]. The grains in the spine are very coarse and the grain boundaries large. The red arrows in Figure 11 indicate the grain boundaries of large grains. At this position, inter-crystalline corrosion can appear. The chemical reaction between lead spines and sulfate acid take place along the direction of extension of the grain boundaries. Therefore, reducing grain size and consequently increasing the length of grain boundaries from the surface to the center of spines is a valid way to increase the work life of a battery.

➢ Oxide

In casting there is a risk of oxide inclusions due to the oxidation of the molten surface. The oxide film which exists at the surface reduces the chemical reaction rate between the spines and battery acid.

3.4   New developments in manufacturing of tubular plates

To avoid the defects of die-casting, a new method for production will be explored: forming at room temperature (cold extrusion).

The advantages of cold forming are well known [14]:

➢ High speed manufacturing reduces production costs
➢ Surface finish is improved in comparison to machined surfaces
➢ Critical and close tolerances can be held
➢ No energy requirement to melt materials
➢ Less or no waste of raw materials
➢ No poison vapor

The tubular plate consists of top bar carrot and lead spines. With the special form and geometry of the plate in mind, the extrusion method is possible.

3.4.1 Introduction of extrusion

Extrusion is a very important forming process used to produce long, straight, semi-finished metal products such as bars, solid and hollow sections, tubes, wires and so on. The principle of extrusion is very simple: a billet is squeezed through a die under a high load in order to reduce its size. Cross sections of varying complexity can be extruded, depending on the material and the dies used. Extrusion can be carried out at room temperature or at higher temperatures, depending on the alloy and the method used.

There are four characteristic differences among the various methods of extrusion and the presses used [15]:

a. The movement of the extrusion relative to the stem: direct and indirect processes
b. The position of the press axis: horizontal or vertical presses
c. Type of drive: hydraulic or mechanical presses
d. Method of load application: conventional or hydrostatic extrusion

The differences in flow characteristics of various metals to be extruded and the complex relationship between extrusion parameters make it impossible to use the same method for all materials. Special methods are used to obtain optimum quality and productivity in accordance to the flow behaviour of the metal under consideration. In addition, production methods are chosen depending on the final product. The two basic methods, direct and indirect extrusion, are illustrated in figure 12.

1 – Billet   4 – Extrusion stem
2 – Container   5 – Dummy block
3 – Die   6 – Die holder
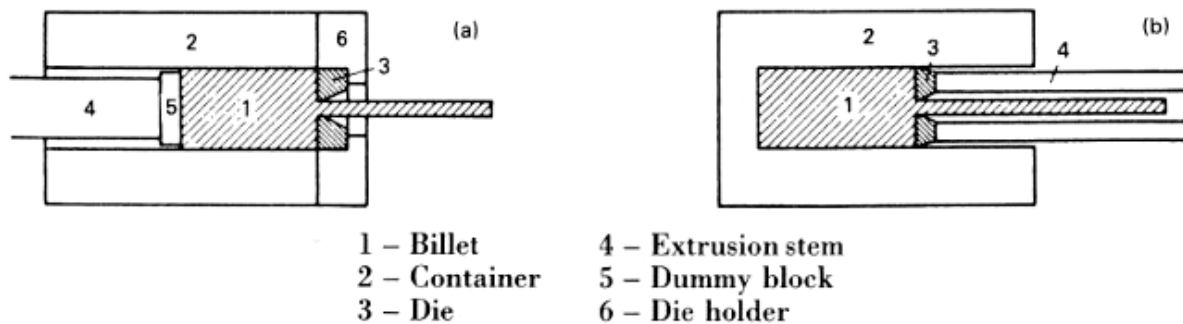
(a) direct extrusion,   (b) indirect extrusion

Figure 12: Basic methods of extrusion [15]

Direct extrusion is one of the most critical as well as common methods for producing extruded profiles. It is typically used for manufacturing solid rods, bars, hollow tubes, solid sections etc. Direct extrusion offers many advantages, for instance cost-effectiveness, simple fastening and assembly and complex integral shapes are possible. The major disadvantage of the direct extrusion process is that the force required to extrude the billet is greater than for indirect extrusion because of the

frictional forces introduced by the need for the billet to travel through the entire length of the container. Consequently, the greatest force is required at the beginning of process and slowly decreases as the billet is used up. At the end of the billet, the force greatly increases because the billet is thin and the material must flow radially to exit the die [16].

During indirect extrusion, the die is held in place by a stem, which has to be longer than the container length. The maximum length of the extrusion is ultimately dictated by the column strength of the stem. Because the billet moves with the container, the frictional forces are eliminated. This leads to the following advantages [16]:

➢ 25 - 30% reduction of friction, which allows for extruding larger billets, increasing speed, and an increased ability to extrude smaller cross-sections
➢ Less tendency for extrusions to crack as there is no heat coming from friction
➢ The container liner lasts longer due to less wear
➢ The billet is used more uniformly so that extrusion defects and coarse-grained peripherals zones are less likely

The disadvantages are as follows [16]:

➢ Impurities and defects on the surface of the billet affect the surface of the extrusion. These defects ruin the product if it is subsequently anodized or the aesthetics are important. In order to get around this issue, the billets may be wire brushed, machined or chemically cleaned before use.
➢ The process is not as versatile as direct extrusion because the cross-sectional area is limited by the maximum size of the stem

3.4.2 Extrusion of the tubular plate of a battery

An alternate manufacturing method to die-casting a tubular plate is the cold extrusion process. Compared to die-casting, extruding a tubular plate involves more steps and is more difficult to control. However, in view of the above-mentioned advantages of forming, a series of tests, described in chapter 5, will be made to evaluate the possibility of using the extrusion method.

In addition, lead is a very soft metal with low hardness and yield strain. That means it is also easy to deform at room temperature. Generally, forming at a temperature lower than that of recrystallization is called cold forming. Technically, due to the very low recrystallization temperature of lead (as low as 0°C), room temperature extrusion for lead officially falls under hot forming. However it is generally referred to as cold extrusion.

4 Raw materials - lead and its alloys

Lead is an important raw material for producing lead-acid batteries. The properties of lead and its alloys as well as their deformation and extrusion characteristics are described in this chapter.

4.1 General Properties of lead

4.1.1 Chemical and physics properties of lead

When freshly cast, lead has a bright silvery appearance, however upon exposure to air, the surface soon turns grey or grayish-white due to the formation of oxide. Basic carbonate or basic sulfate films protect the surface form further corrosion in most atmospheres [17].

Lead is the softest of the common metals and because of its high ductility and malleability, can be easily formed into complex shapes without the frequent annealing and softening steps required by many other metals. The physical and atomic properties of lead are summarized in Table 1 and Table 2.

Property	Value
Chemical symbol	Pb
Color	Light grey to a slight bluish grey
Crystallographic structure	Face-centered cubic
Melting point	327.4 °C
Boiling point	1725 °C
Density at 20C	11.336 g/cm^3
Specific gravity	11.3
Tenacity	Malleable, ductile

Electric resistivity	$212*10^{-9}$ $\Omega \cdot m$
Hardness	1.5 (Mohs); 38.3 MPa (Brinell)
Young's Modulus	16 GPa
Shear modulus	5.6 GPa
Bulk modulus	46 GPa

Table 1: Physical properties of pure lead [18]

Property	Value
Atomic number	82
Atomic mass	207.2 u (1u=1.0003179 amu)
Atomic radius	1.47 Å
Covalent radius	1.81 Å
Atomic volume	18.17 cm^3/mol
Stable isotopes	4
Electro negativity	2.33

Table 2: Atomic properties of pure lead [18]

4.1.2 Health and safety issues by lead and its alloys

As with many elements used in high technology, a health hazard posed by lead is a concern. Lead and its compounds are cumulative poison and should be handled with recommended precautions. These materials should not be used in contact with food and other substances that may be ingested.

Lead can damage nervous connections (especially in young children) and cause blood and brain disorders. Lead poisoning typically results from ingestion of food or water contaminated with lead; but may also occur after accidental ingestion of contaminated soil, dust, or lead based paint [34]. Long-term exposure to lead or its salts (especially soluble salts or the strong oxidant PbO_2) can cause nephropathy, and colic-like abdominal pains. The effects of lead are the same whether it enters the body through breathing or swallowing. Lead can affect almost every organ and system in the body. The main target for lead toxicity is the nervous system, both in adults and children. Long-term exposure of adults can result in decreased performance in some tests that measure functions of the nervous system. It may also cause weakness in fingers, wrists, or ankles. Lead exposure also causes small increases in blood pressure, particularly in middle-aged and older people and can cause anemia. Exposure to high lead levels can severely damage the brain and kidneys in adults or children and ultimately cause death. In pregnant women, high levels of exposure to lead may cause miscarriage. Chronic, high-level exposure have shown to reduce fertility in males. The antidote/treatment for lead poisoning consists of dimercaprol and succimer [35].

4.2 Lead alloys

Lead, very soft and ductile, is normally alloyed with antimony, tin, arsenic and calcium. The alkalis and alkaline earth elements have a greater effect on the hardness at similar concentration, but these alloys are not of much industrial interest.

Alloying additions are made to improve mechanical and electrochemical properties of lead-acid battery grids and spines. The Pb-Sb-based ternary alloys with As, Sn, Ag, Se, Cu, S and Pb-Ca-based ternary alloys with Sn, Ag, and Al have been considered in grid alloys for batteries. In the early battery grids, Sb was the main alloying element used and up to 11%Sb was used. By 1950, the phenomenon of Sb poisoning of the negative plate was recognized and the Sb content was decreasing, with 6~9% Sb alloys becoming common. However, the low-Sb alloys had inferior cast ability, mechanical strength and corrosion resistance under battery operating conditions. Arsenic addition increased the rate of age hardening and reduced the time of grid storage required after casting. The Sn addition increased fluidity and thus cast ability. It increased cycle life of batteries containing thin plates [19]. Ag additions increased both the corrosion and creep resistance in Pb-Sb-alloy grids. The disadvantage was the high cost of Ag.

Therefore the following alloys will be discussed as they play an important role in the battery industry: the lead-antimony alloy, lead-tin alloy, lead-antimony-tin alloy and lead oxide.

4.2.1 Lead-antimony alloy

Antimony is the most common alloying element used to increase the hardness of lead for practical applications. Lead-antimony alloys known simply as hard lead are used extensively and as such represent the most important group of alloys for pipes and sheets, cable sheathing, collapsible tubes, storage battery grids and anodes. The

alloys are grouped in the German standard specification DIN 17641 of 1962 lead-antimony alloys (hard lead) [19].

The lead antimony diagram has recently been revised by RAYNOR [20] on the basis of a critical survey of the literature.(Figure13) According to this source, the eutectic temperature is to be taken as 252°C and its composition as 11.1% Sb. According to DASSOJAN [21], addition of 0.1% of ebonite to lead-antimony storage battery alloys refines the structure (owing to the sulfur content of the ebonite) and improves the casting ability. As lead can take up a maximum of 3.45%Sb in solid solution, alloys with lower antimony contents should contain no eutectic.
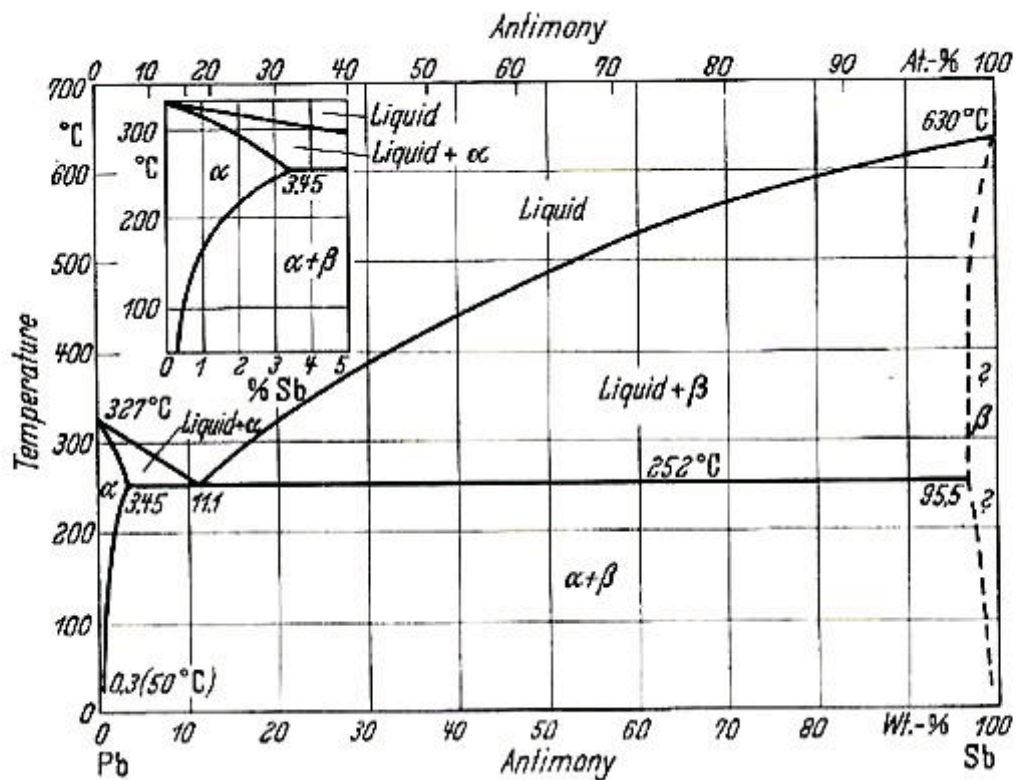
Figure 13: Lead-antimony. (According to RAYNOR) [20]

The antimony contents of the lead alloy can range from 0.5 to 25% depending on the field of application. The hardness of antimony lead increases greatly with increasing antimony content up to the eutectic composition. Table 3 shows how the characteristics hardness and strength vary according to antimony content. For this

reason, alloys with 3 to 11% Sb are normally used to cast of thicker cross-sections, such as connectors of framed plates or battery plates.

Antimony (%)	Tensile strength(N/mm)	Hardness (HB)
1	23,46	7,0
2	29,00	8,0
4	39,05	10,1
6	47,20	11,8
8	51,20	13,3
10	52,92	14,6

Table 3: Mechanical properties of some cast lead-antimony alloys [20]

The alloys with higher antimony content have the advantage of better casting fluidity, but the disadvantage of resulting in a higher self-discharge of the battery. At an antimony content of 10%, the electrical conductivity falls by 23% of the value for pure lead [22].

Furthermore, high antimony content of battery grids can aggravate the consumption of water in battery acid, leading to a shorter battery service life [5].

4.2.2 Lead-tin alloy

In storage, the lead-tin alloys do not assume the grey appearance of soft lead. The difference is already recognizable with a tin content of a few percent. Lead-tin shares with lead-antimony the role of being the most important alloy group of lead. Tin contents up to 3% are used for cable sheathing. Along with other alloying elements, principally antimony, tin is an essential component of bearing metals, which exemplify multi-metal alloys.

The phase diagram shown in figure14 was derived from a critical evaluation of various investigations up until now [23]. According to this phase diagram the solubility of tin in lead at room temperature amounts to approximately 1.3%.
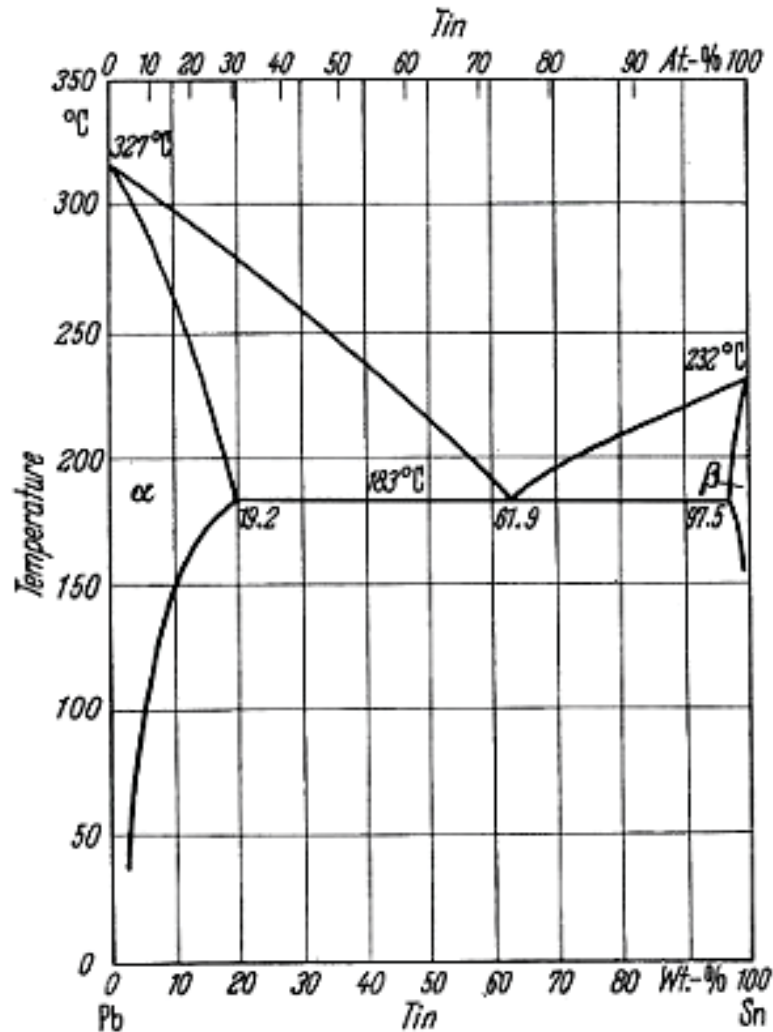
Figure 14: Lead-tin phase diagram [24]

As can be seen in Table 4 and above Figure14, the 62% tin lead alloy results in the maximum tensile strength, shear strength and impact strength. The 62%-tin composition is also known as the eutectic point of the alloy, where the alloy behaves

like a pure metal having a single melting (solidification) temperature (176℃). The hardness and electrical conductivity increase with increasing tin content.

For the battery industry, a hardness exceeding 14 HB is required for the electrode grids [2]; the higher the hardness and conductivity the better quality of grids. Suitable tin contents can therefore not only increase the hardness of electrode grids, but also improve the electrical conductivity.

Moreover, Figure15 shows the age hardening of lead alloys with different tin contents. Thus a lead alloy with 1.3% tin content, which is aged at room temperature for 60 or 70 days, can acquire the required hardness [5].

Tin (wt.%)	Electric resistivity (Ω·m)	Thermal conductivity (W/m·K)	Tensile strength (MPa)	Shear strength (MPa)	Elastic modulus (GPa)
0	212	34.8	12	12	18
5	207	35.2	28	14	18.5
10	204	35.8	30	17	19
20	192	37.4	33	20	20
40	166	43.6	37	32	23.7
60	145	49.8	52	36	30
63	144	40.9	54	37	31.5
70	134	30.3	54	36	35

Table 4: The properties of lead-tin alloys [19].

The Hardening of Pb-Sn alloys at room temperature
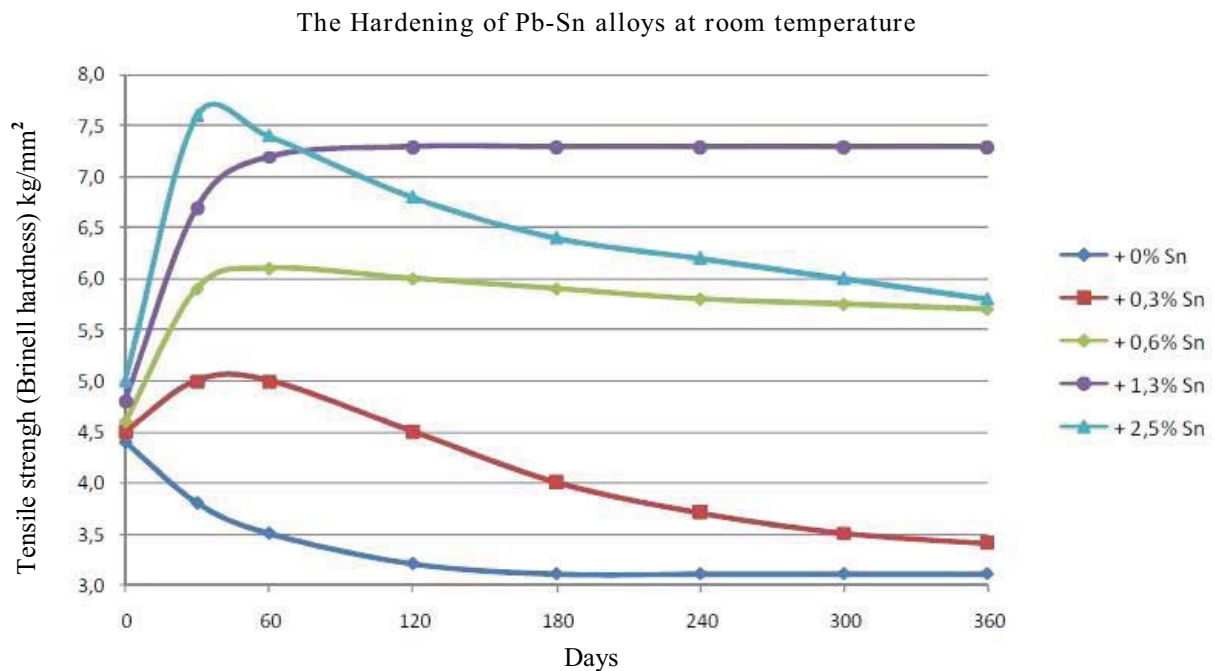
Figure 15: Change in hardness of lead-tin alloys after aging [5].

4.2.3 Lead-Antimony-Tin Alloy

This ternary system is the basis of a series of important lead alloys and notably type metals. The alloys with lower concentrations of tin and antimony are used in cable sheathing and battery grids.

The phase-diagram (Figure 16) was devised by V.LOEBE [24]. As no ternary compound exists, the diagram only contains the crystallization fields of the boundary system phases, i.e. of lead, antimony, tin and of their solid solutions in one another (including the two phases β and β´ of the antimony-tin-system). As β and β´ correspond approximately to the formula SbSn, with an excess of antimony or tin respectively, and presumably have very similar crystal structures, they can be regarded at a first approximation to be one single phase [25]. According to Figure16 the liquid surface of the diagram is crossed by a eutectic trough, which runs form point E1 of the lead-antimony system to the lead-tin eutectic, E3.
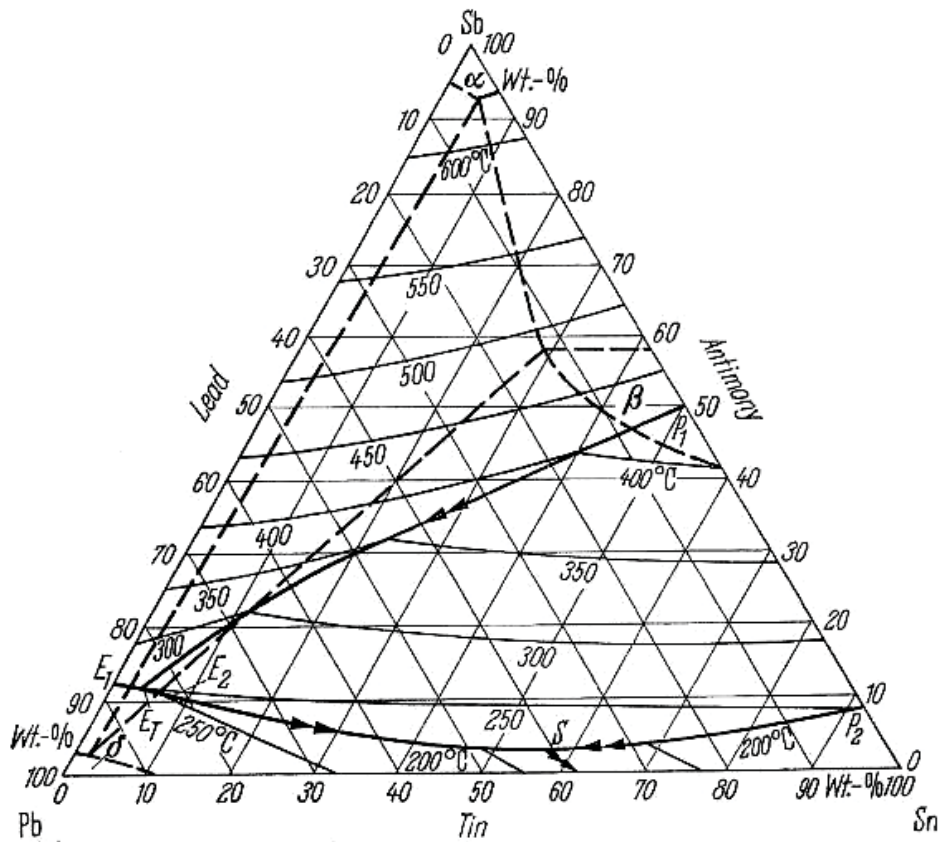
Figure 16: Lead-antimony-tin phase diagram [24]

A peritectic trough corresponding to the equilibrium, Melt + β ⇔ γ, starts from point P_2 of the antimony-tin system and meets the eutectic trough mentioned above at S point with 57.5% Sn, 2.5%Sb, 40%Pb and 189 ℃. S is the corner point of a peritectic four-phase plane with the reaction, Melt S + β ⇔ γ(tin) + δ. The trough P_1-E_T largely represents, according to Figure 16, the reaction, Melt + α = β, but in the neighborhood of E_T assumes a eutectic character, corresponding to the reaction Melt ⇔ α + β, which can be recognized by a change in the direction of the tangent. The trough E_T E_2 rises up at E_2 and then falls steadily to a point S and E_3. E_2 heaving the composition 10% Sb, 10% Sn at the temperature 246.5℃ , signifies a quasi-binary eutectic of lead with SbSn [24].

4.3 Lead oxide

Lead oxide may refer to lead (II) oxide-PbO, lead (II, II, IV) oxide-Pb_3O_4 or lead dioxide (lead (IV) oxide)-PbO_2.

Lead (II) oxide is the chemical compound with the formula PbO. Lead (II) oxide occurs in two forms. The first is red in color and tetragonal crystal in structure. The second form is yellow in color and has an orthorhombic crystal structure [20]. PbO is the main component of the paste used to fill the plates during the manufacturing of lead-acid batteries.

Lead dioxide is also named plumbic oxide and lead (IV) oxide, with lead in oxidation state +4. It has a molar mass of 239.2 g/mol and occurs in nature as the mineral plattnerite [19]. The most important application of lead dioxide is as the cathode of lead acid batteries.

Two important modifications of lead dioxide are α-PbO_2, and β-PbO_2. As the α-form is thermodynamically less stable than the β-form, some transformation of α-PbO_2 into β-PbO_2 may occur during the life of a battery, with consequent improvement in its performance. The positive plates, which still possessed their nominal capacity, consisted of hard branched crystals of α-PbO_2. The β-PbO_2 was embedded between these crystals. The crystalline structure of α-PbO_2 determines the strength of the plates, while the active β-PbO_2 principally controls the capacity of the battery. In batteries with a capacity below 50% of the nominal, the plates consisted only of β-PbO_2 [19].

 The lead oxide is produced by either the ball mill process or the Barton Pot process [33]. In the ball mill process, the grinding action on high-purity lead feed results in fine particles of partially oxidized lead. The particles are removed by the airstreams and collected in a cyclone. The irregularly shaped platelets with a mean size of 3~4

μm and containing up to 25~30% un-oxidized lead are obtained. In the Barton Pot process, the lead oxide is produced by the oxidation of fine molten lead droplets thrown up by the agitation of the pure molten lead holding pot. The airstreams carries the particles to a cyclone, where they are collected. The Barton Pot oxides are spherical in shape with a mean size of 7~8 μm and un-oxidized lead content of up to 40%.

4.4 Mechanical properties of lead and lead alloys

As mentioned earlier in this chapter, lead is normally used at temperatures much closer to its melting point than most common metals and in consequence is subject to recrystallization at low stresses. The results of mechanical tests such as hardness, E-module and yield point are therefore affected by the rate of application of the stress. The Brinell hardness of pure lead, usually quoted, lies between 4 and 6, making it the softest of the common metals and thus extremely malleable [19].

The mechanisms by which plastic flow of a metal or material occurs involve processes occurring on the atomic scale that include the glide motion of dislocation lines, the coupled glide and climb of dislocations, the diffusive flow of individual atoms, the relative displacement of grains by grain boundary sliding, and mechanical twinning that involves the motion of twinning dislocations, at all temperature above 0 K, thermally activated movement of atoms and dislocations is present. The extent of thermal activation increased with the homologous temperature (T/T_M), where T is the temperature of interest and T_M is the melting point. The low melting point of lead and lead alloys makes the contribution of thermal activation to plastic flow very significant, even at room temperature, which corresponds to homologous temperature of around 0.5 K [21]. The evaluation of mechanical property data on lead and lead alloys requires an appreciation of the different mechanisms of plastic flow that are operative at room temperature and at elevated temperature, to which lead alloys will be subjected.

The considerable dependence of tensile strength on the duration of test is paralleled by a similar relationship of temperature. According to determinations by W.HOFMANN and co-workers [37], the tensile strength at -183 ℃ is about twice as great as at 20 ℃. The following data in Table 5 shown the tensile strength in the

range between room temperature and 265 ℃. The tensile strength increases (as in other metals) with decreasing grain size. Therefore, the material need to be extends to smaller grain sizes.

Temperature [℃]	20 ℃	82 ℃	150 ℃	195 ℃	265 ℃
Tensile strength [MPa]	13.23	7.84	4.9	3.92	1.96
Elongation [%]	31	24	33	20	20

Table 5: Tensile strength of pure lead by different temperatures [19].

Besides, values for the cohesive strength ＝ separation strength of lead, can be obtained if the plastic elongation and contraction in the tensile strength are hindered. This is possible by the use of cold pressure welding. After welding, the thickness of lead (or lead oxide) layer was a few multiples of 0.1 mm. On applying a tensile stress, an inhomogeneous tri-axial state of tensile stress is present in the lead. Fracture occurs in the lead. The value of the cohesive strength, about 4 kg/mm^2, thus determined can only be regarded as a guide [19].

4.4.1 Deformability behaviors of lead and lead alloys

The deformation of cubic face-centered metals, to which lead belongs, takes place by sliding along the octahedral planes {1 1 1}. There are six slip directions ⟨1 1 0⟩ in each of four possible octahedral slip planes. As with all other face-centered cubic metals, micro sections of re-crystallized lead show twinning lamellae. These are cases of coherent twins according to the Spinel Law [19].
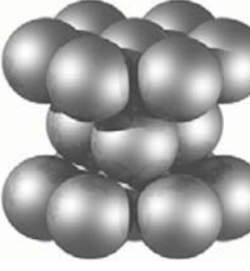
Crystal structure	Example	Slip plane	Slip direction	Slip system	Deformability
Face-centered cubic	Pb Al Cu….. γ-Fe	4	3	12	Very good
Body-centered cubic	Cr, Mo α-Fe	6	2	12	good
Hexagonal	Zn, Be	1	3	3	Poorly

Table 6: Crystal structures and their deformability [17].

The Table 6 shows the typical crystal structure of metal. Metals with face-centered cubic structures or body-centered crystal structures have a relatively large number of slip systems. These metals are quite ductile because extensive plastic deformation is possible along the various slip systems [30].

The ease of deformation is controlled by the flow stress k_f under the given conditions and the degree of deformation by the ductility φ_{Fr}. Thus workability can be expressed as equation 1 [26]:

$$W \approx \varphi_{Fr} / k_f \qquad\qquad\qquad (\text{ Eq.1})$$

The workability provides a relative value for the extrusion ability. The relationship between the φ_{Fr} / k_f ration and extrusion ability is not particularly accurate, but the following classifications serve as a practical guide:

φ_{Fr} / k_f		Extrude ability
<2	……………………………………………	Poor
2 to 4	……………………………………………	Average
4 to 15	……………………………………………	Good
>15	……………………………………………	Very good

Table 7: The classification extrusion ability [26].

It must be emphasized that this refers only to the extrusion ability of the material and does not indicate whether a certain section or tube can be produced from a material with good extrusion ability. In other words, even though the metal lead has very good extrusion behavior, extrusion parameters (e.g. temperature, extrusion ratio, billet length, etc.) can be so unfavorable that the available press capacity is

insufficient [11]. Therefore, generally speaking, though pure lead is very easy to extrude, the extrusion ability must still be assessed for each individual case.

4.5 Extrusion characteristics of lead and lead alloys

As mentioned above, lead and lead-based alloys exhibit high ductility and are easy to extrude. The addition of alloying elements increases the required force for extruding. Pure lead has a very low flow stress as shown in Figure 17. It is, therefore, not possible to draw pure lead to wire. However, lead alloys have higher flow stresses. Addition of Sb and Sn produce solid-solution hardening of the lead, increasing both the base strength the work hardening capability. This raises the recrystallization temperature. The loads needed in deformation processes also increase. Thus, the principal applications of lead alloys include pipes, wire, tubes and sheathing for cable.
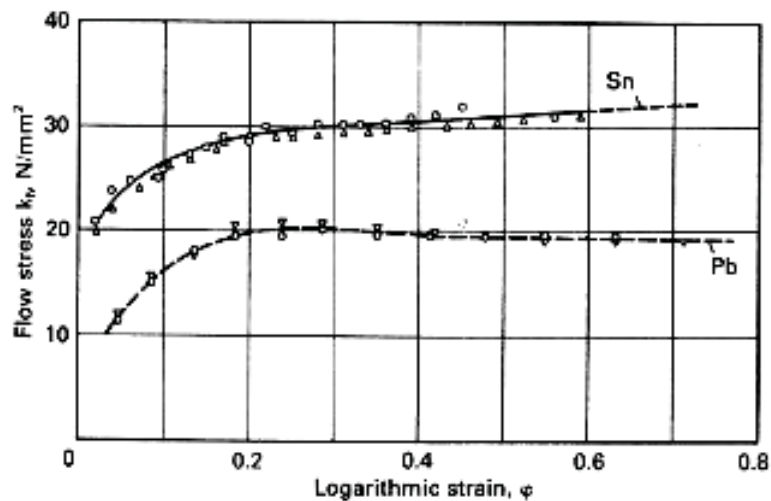
Figure 17: Stress-strain curves of lead and tin at room temperature [19].

Rod and wire for solders are usually extruded using a direct method, that is, by the ram of the press pushing the metal through a die. Multi-hole dies are often used for small diameter wires of about 1~5mm diameter [18]. With most other extruded lead products it is common practice to pour molten metal into the container of the press

allowing it to solidify before extrusion takes place. However, for rod and wire it is more common to use pre-cast billets, especially for solder alloys.

4.5.1 Flow type of lead and its alloy during extrusion

Normally, the flow process in extrusion can be made visible in different ways, for instance, by using, as model materials, wax billets having layers of different colors, or alloy billets having layers of somewhat varied composition, which contrast with one another on etching. On the basis of such method, PEARSON [36] distinguishes four kinds of flow in the extrusion process.

Type S is based on the assumption of negligible friction between the billet and the container as well as between the billet and the die front surface. But it is purely theoretical and does not occur in practice.

Type A is characterized by the fact that friction between the outside of the billet and the container is excluded or at least extensively reduced by using inverted extrusion or , in the case of direct extrusion, by a lubricant. Type B consists of those extrusion processes in which friction works itself out fully on the skin of the billet. In that case the skin remains adherent to the container and is sheared off the bulk of the billet. The meshes of the network on the periphery of the emerging extrusion are therefore much more distorted than in Type A. Type A and B occur principally in low-melting metals, and lead and its alloys flow in direct extrusion with the flow Type A.

Type C is, on the contrary, found in extrusion processes which take place at high temperatures, for instance in the extrusion of copper. Here the outside of the billet cools considerably; first of all therefore, the warmer internal zones flow within a thick peripheral layer. Only afterwards does the latter take part in the flow process.

Lead has even better bearing properties than tin. Lead alloys, therefore, also flow mainly according to flow type A in direct extrusion.
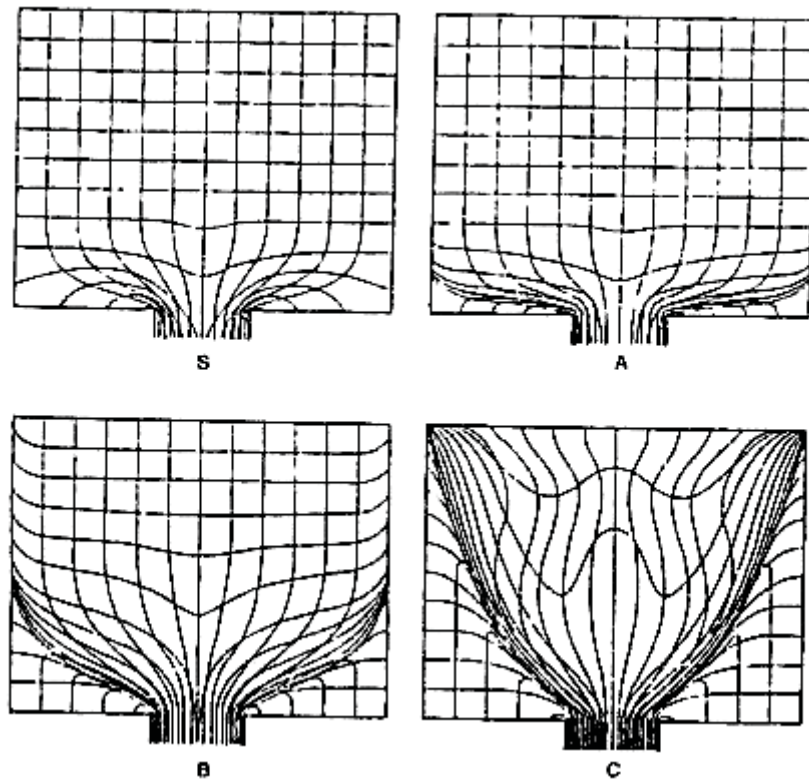
Figure 18: Extrusion flow patterns [36]

Lead alloys will weld during extrusion at suitable temperatures and extrusion pressures similar to tin alloys and certain aluminum alloys. Tubes or hollow sections can, therefore, be extruded with pothole and bridge dies. Feeder chamber dies have also proved successful for the extrusion of these materials and are require for billet-on-billet extrusion. The tools used for the extrusion of lead alloys are in principle similar to those used for aluminum extrusion, although the designs are simpler because of the significantly lower thermo mechanical stresses.

5 Experimental method

5.1 Experimental equipment used

The compression tests were carried out on a SERVOTEST thermo-mechanical treatment simulator (TMTS) as shown in figure 19. The extrusion tests were carried out on an old WERNER & PFLEIDERER hydraulic 4-columm-press machine shown in figure 20. The hardness testing of materials were carried out on an EMCO-TEST M1C 010 and using the Brinell "HB" Scale.

Figure 19: Thermo-mechanical treatment simulator

Figure 20: Hydraulic 4-column-press machine

5.2 Macrostructure and hardness of tested material

The materials used for this investigation were supplied by BM-battery machine GmbH. Two kinds of raw material ingots were used, one was 99.9% pure lead and another was a lead-antimony alloy. The composition of pure lead and the lead-antimony alloy can be seen in Table 8 and Table 9. Before performing the extrusion test, properties such as hardness and grain size of the raw material were documented for reference purposes. The internal crystal structure of the tested materials could therefore be compared with the crystal structure after the compression tests and extrusion tests respectively.

Pure lead							
Pb %	Sb %	Sn %	As %	Ag %	Bi %	Ni %	Zn %
99.985	0.002	0.001	0.001	0.001	0.01	-	0.001

Table 8: Metal composition of pure lead.

Lead-antimony alloy							
Pb %	Sb %	Sn %	As %	Ag %	Bi %	Ni %	Zn %
96,264	3.5	0.1	0.09	0.026	0.0127	0.0015	0.005

Table 9: Metal composition of lead-antimony alloy.

Specimens were taken from the ingots for investigation by means of a fret-saw, cooled by alcohol. The surface of the micro-section was prepared by filing, turning

or planing. Thus the deformed surface layer must be completely removed by subsequent grinding and etch polishing.

First, the specimens were hand-ground on a grinding/polishing machine with P220 emery paper (wheel speed: 150-250 rpm, 15 minute emery) followed by P600 (wheel speed: 150-250 rpm, 15 minute emery) and P1200 emery paper (wheel speed: 150-250 rpm, 25 minute emery). Carnauba wax was used to prevent the lead from smearing and emery from being embedded in the surface. Then the specimens were polished with 9µm and 3µm polishing paper (wheel speed 150-250 rpm), cooling water and polishing medium until large scratches disappeared and the surface of the specimen was reflective. As not all scratches disappeared during this polishing, a finer polishing was carried out on a slow wheel with 0.25µm polishing paper (wheel speed: 120-150), cooling water and polishing medium.

1. Pure Lead (99.99%).
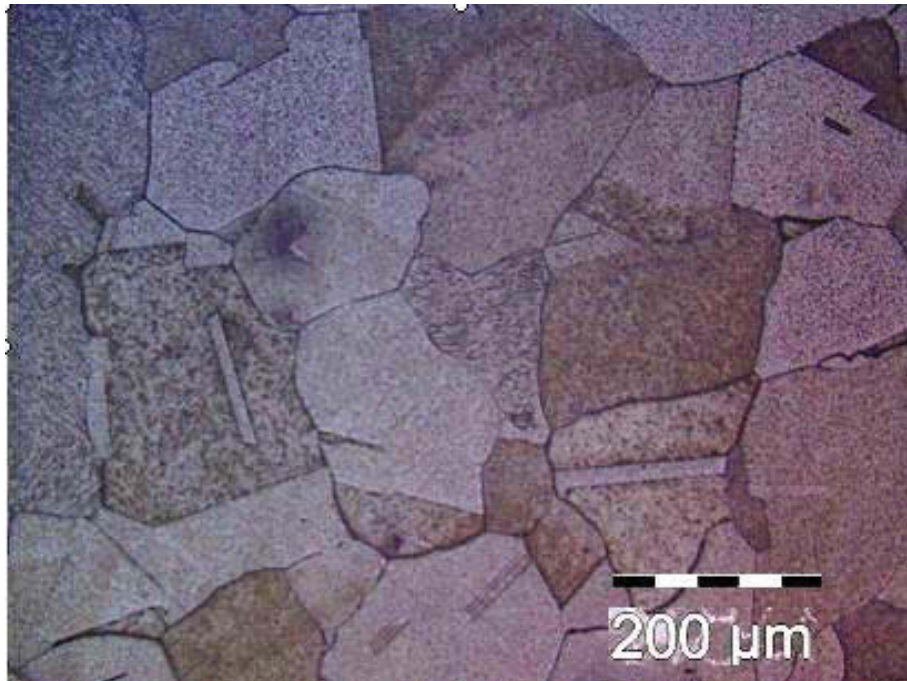
Figure 21 a Micrograph of pure lead after etching

Etching media for lead and lead alloys: standard Villa etching medium:16cm^3 nitric acid(1.4%), 16cm^3 Glacial acetic acid, 68cm^3 glycerol [20].

2. Lead-antimony alloy （Sb: 3.5%）
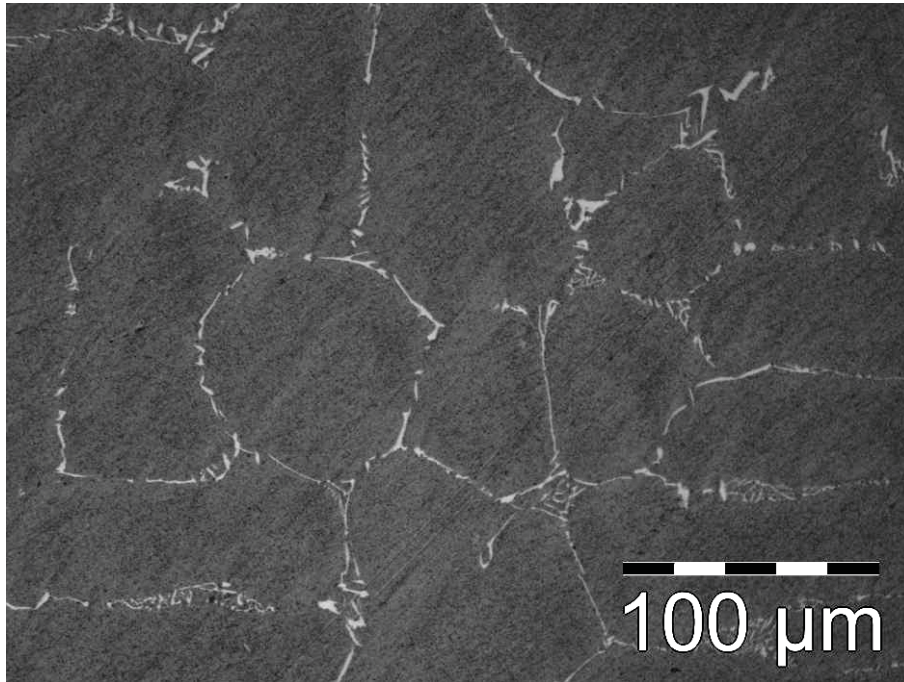
Figure 21 b: Micrograph of lead alloy after etching

Ground mass is lead solid solution and with antimony eutectic existing at the grain boundaries

The final step was removing the oxide skin with VILELLA solution mixed with a solution of three parts glacial acetic acid and one part H_2O_2 (30%). The fully polished specimens were then washed with pure alcohol and dried with hot air. The finished surface of the specimens, sensitive to touch and tarnishing, were examined shortly thereafter and photomicrographs made. Figure 21 a and Figure 22 b show the above mentioned micrographs of the lead and lead-antimony alloy specimens prepared.

The hardness and grain size of the specimens are noted in Table 10, whereby ECD stands for equivalent circle diameter. D_{max} and D_{min} denote the average maximum and minimum diameters of the grains. These results show that pure lead has a much larger grain size and lower hardness compared to the lead-antimony alloy.

	HB	ECD	Elongation	D_{max}	D_{min}
Pure lead	6.2	132.7	1.42	202.73	83.61
Lead alloy	13.6	77.2	1.89	113.79	67.32

Table 10: Brinell hardness and grain parameters

ECD: equivalent circle diameter

Dmax: average maximum grain size

Dmin: average minimum grain size

5.3 Compression tests

The plastic deformability of a metal is described by its flow curve and ductility as a measure of the forming limits. The most frequently applied methods for determining flow cures are tensile tests, compression tests and torsion tests. Normally the formability of metals is lowest under tensile hydrostatic stress. Therefore higher strains are obtained by compressive tests than by tensile tests.

5.3.1 Test parameter

According to the DIN 50106, the specimens of compressive tests are circular cylinders, with length to diameter (L/D) ratios of 1.5~2 (Rastegaev specimen). Therefore, compression tests were performed on lead and lead-antimony alloy using work pieces of 16mm in diameter and 24mm in height. Figure 22 shows such a specimen.

Figure 22: Specimen for compression testing

The cylindrical specimen was placed between compressive plates parallel to the surface. Graphite paste was used for lubrication [27]. Compression was applied at a constant strain rate $\dot{\varphi}$ of 1/s. Compression tests were performed at five different test temperatures: room temperature (approx. 25°C), 50 °C, 100 °C, 150 °C and 200 °C. During the tests, maximum loads were recorded along with stress-strain data.

5.3.2 Test results and discussion

5.3.2.1 Flow curve of pure lead and lead-antimony alloy

Compression readings and corresponding loads were recorded. Figure 23a and 23b show the true stress-strain curve for lead and lead-antimony alloy at different temperatures. This curve is frequently called a flow curve because it shows the stress required to cause the metal to flow plastically at a given strain.
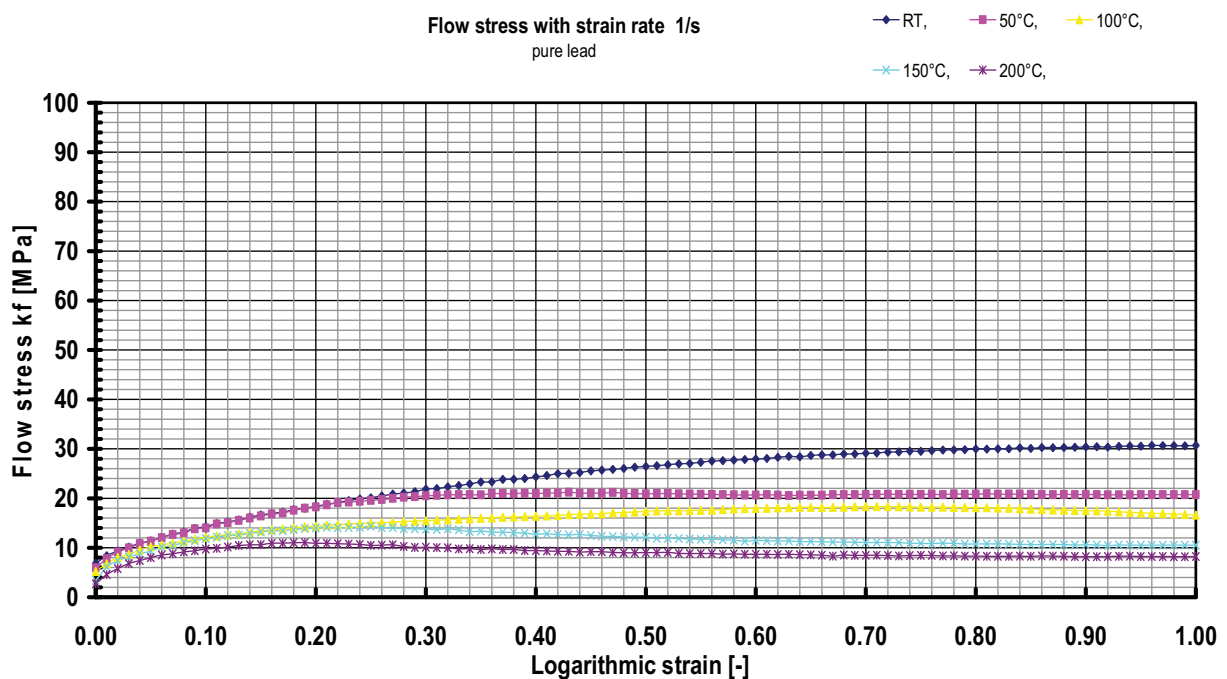
Figure 23a. Flow curve of pure lead at a strain rate of 1/s and at various temperatures
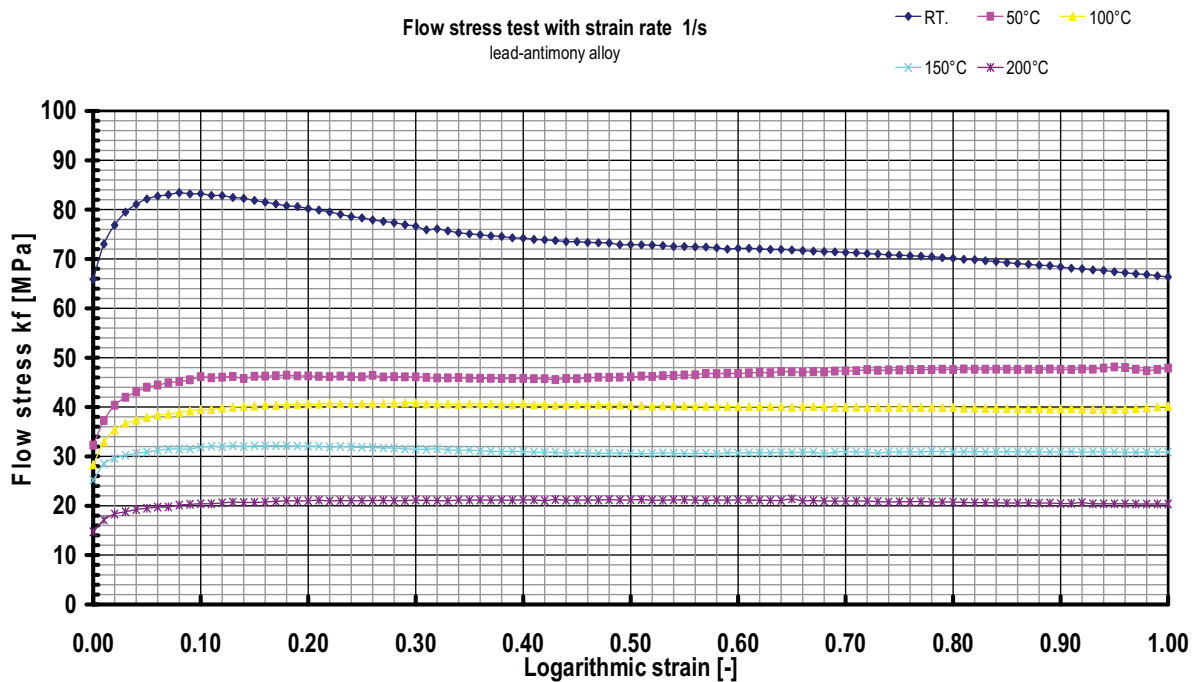
Figure 23 b. Flow curve for lead-antimony alloy (3.5% Sb) at a strain rate of 1/s and at various temperatures

As can be seen in Figure 23 a and 23 b, flow stress decreases with increasing temperature. For pure lead, the flow stress was 32MPa at room temperature; by 200°C it decreased to 10MPa. The flow stress of the lead-antimony alloy on the other hand was higher than pure leads at each temperature. At room temperature, the flow stress of alloy was approximately 76MPa and reached the lowest flow stress, 20MPa, at 200°C.

5.3.2.2 Grain size following the compression tests

The specimens were flat cylinders following the compression tests, as can be seen below. As microstructure has a significant influence on a material's properties, it was important to determine the grain size and state of interior microstructure after forming. Figure 24 indicates the cross section cut for investigating the microstructure of the specimen.

Figure 24: Specimen after compression

Following pictures (in Figure 25 summarized) show the microstructures of pure lead and lead-antimony alloy (3.5% Sn) specimens after compression. The deformation of grains increases with increased temperature.

The lead-antimony alloy shows an elongation of grains along the direction of the compression force. When the temperature reaches 200 °C, grain boundaries become less defined and grains are difficult to differentiate. As Figure 25 (f) shows, the fibers form structure can only be detected.

The grains of pure lead become finer with increasing temperature. Twins appear in the microstructure of the specimen tested at 200 °C.
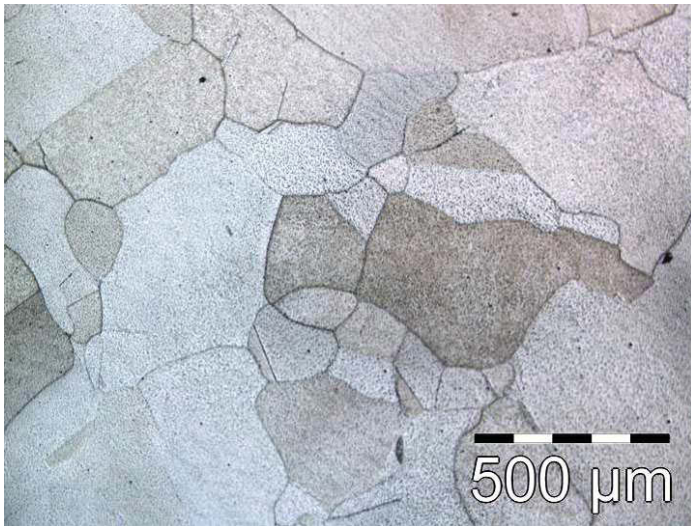
Pure lead   **Lead alloy**
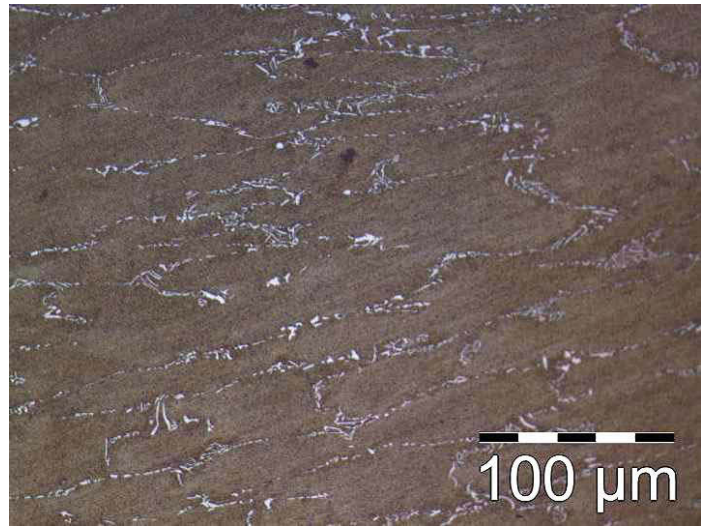
(a) and (b): Compression at room temperature
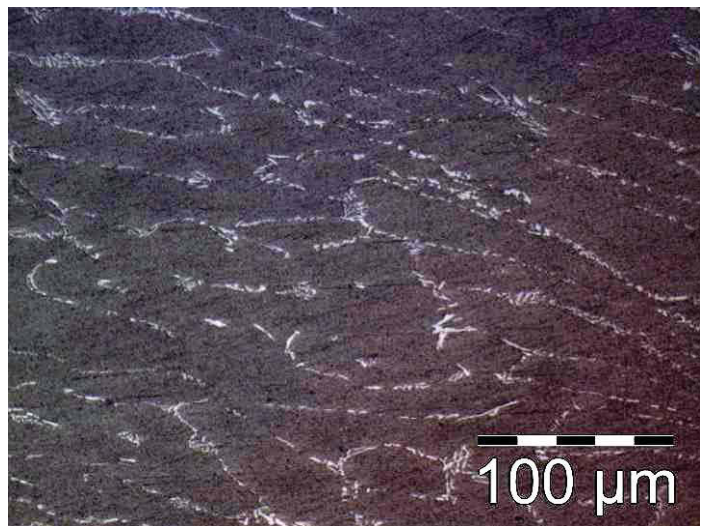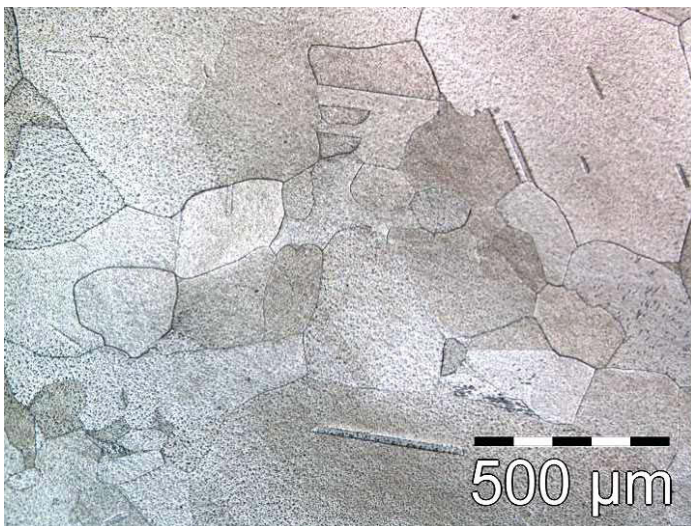
(c) and (d): Compression at 50°C
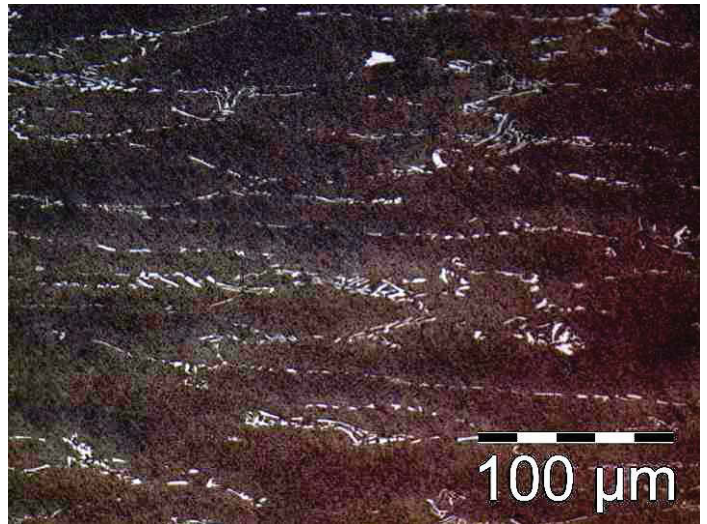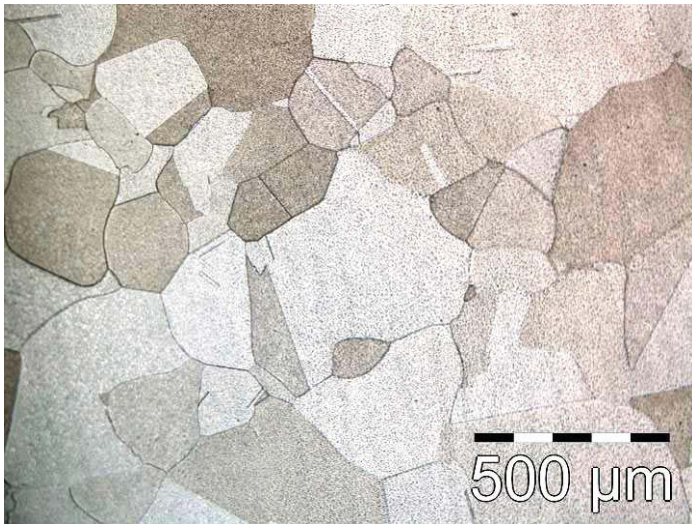
(e) and (f): Compression at 100°C
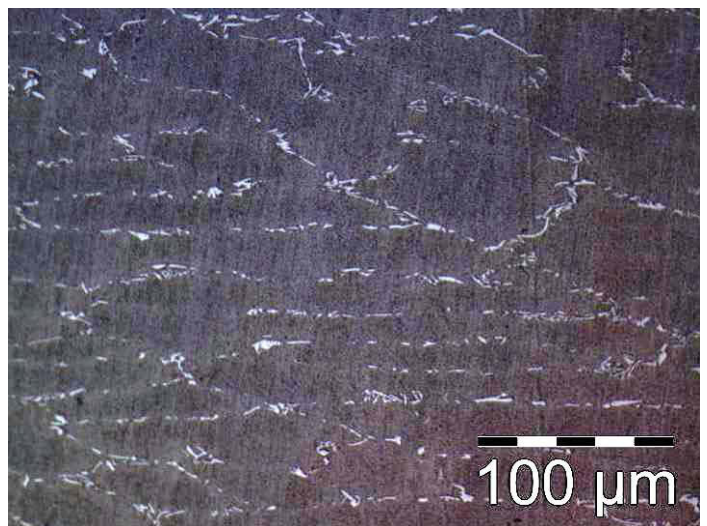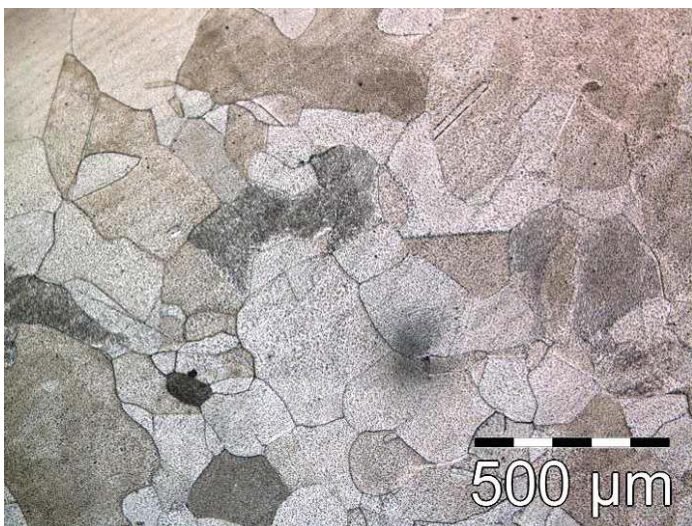
(g) and (h): Compression at 150°C
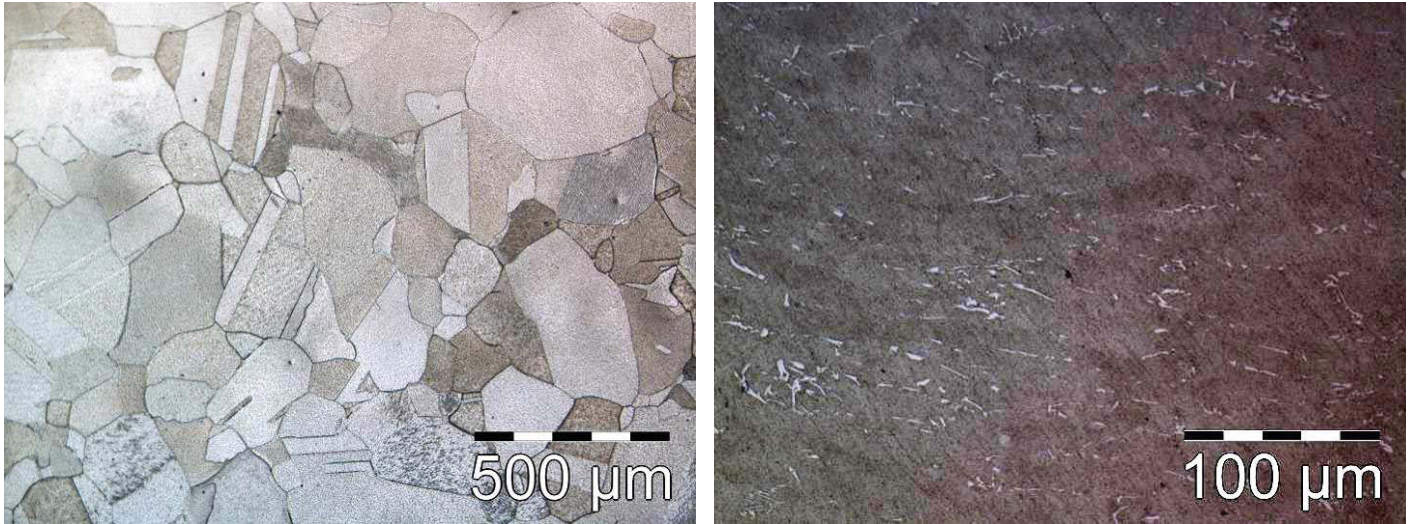
(i) and (j): Compression at 200°C

Figure 25: The microstructure of specimens deformed during compressions test at various temperatures

Table 11 summarizes the grain size parameters and hardness of pure lead and lead-antimony alloy following compression tests. It follows that the hardness of specimen increases according to increased temperatures. At the same time grain sizes decrease. Compared to the grain structure before deformation, the grains of lead and lead-antimony alloy became smaller.

Pure lead					
	HB	ECD	Elongation	Dmax	Dmin
RT	8.4	167.86	1.77	286,29	240.57
50°C	8.8	155.68	1.95	219.77	219.77
100°C	9.2	155.94	1.67	228,81	228.81
150°C	11.3	131.06	1.91	211.04	211.04
200°C	10.1	136.87	1.77	197.56	190.69

(a) Pure lead

Lead-antimony alloy (3.5% Sb)					
	HB	**ECD**	**Elongation**	**Dmax**	**Dmin**
RT	12.3	63.78	4.14	139.52	49.49
50°C	13.1	62.53	2.55	110.41	53.67
100°C	14.2	60.13	4.28	131.12	44.41
150°C	14.4	63.22	4.29	142.32	40.45
200°C	13.3	/	/	/	/

(b) Lead-antimony alloy

Table 11: Crystal parameters and the Brinell hardness following compression

ECD: Equivalent circle diameter

Dmax: average maximum grain size

Dmin: average minimum grain size

5.4 Extrusion tests

The flow stress of lead and lead-antimony alloy at room temperature are now known as a result of the compression tests. Metals with low flow stress are easy to extrude. Hence, lead and lead-antimony alloy billets were extruded at room temperature. Thereafter, the product quality and microstructures of the extruded specimens were investigated.

5.4.1 Test parameter and extrusion model

Choosing a suitable extrusion method for the test was an important first step. Indirect extrusion has a 25% to 30% reduction in load compared with direct extrusion. SIEBEL and FANGMEIER [28] performed the following extrusion tests with pure lead: the movement of the stem was kept constant during the extrusion of lead in a container and the course of pressure was observed over time. They found that the pressure was scarcely higher using this method than when the container wall, die and billet of the inverted press are well lubricated. A further plus is the convenience of the direct extrusion. Taking these facts into consideration, the choice was made to perform the extrusion tests with direct pressure.

The extrusion tests were performed on the hydraulic 4-columm-press machine. The extrusion model, shown in figure 26, was designed to extrude lead and lead-antimony alloy billets. The container wall, die, stem and billets were cleaned and lubricated before commencing with testing. The die was carefully placed in the recess of the die holder.

The diameter and height of the container are as follows: $D_0 = 42.5$mm and $L_1 = 100$mm. Extrusion tests were conducted at room temperature with an average stem (punch) speed of 4.6 mm/s. Billets with length of 75 mm and a diameter 40 mm were extruded. In the course of extrusion, the material was formed from a diameter of 40mm to 10mm and then from 10mm to 3mm.
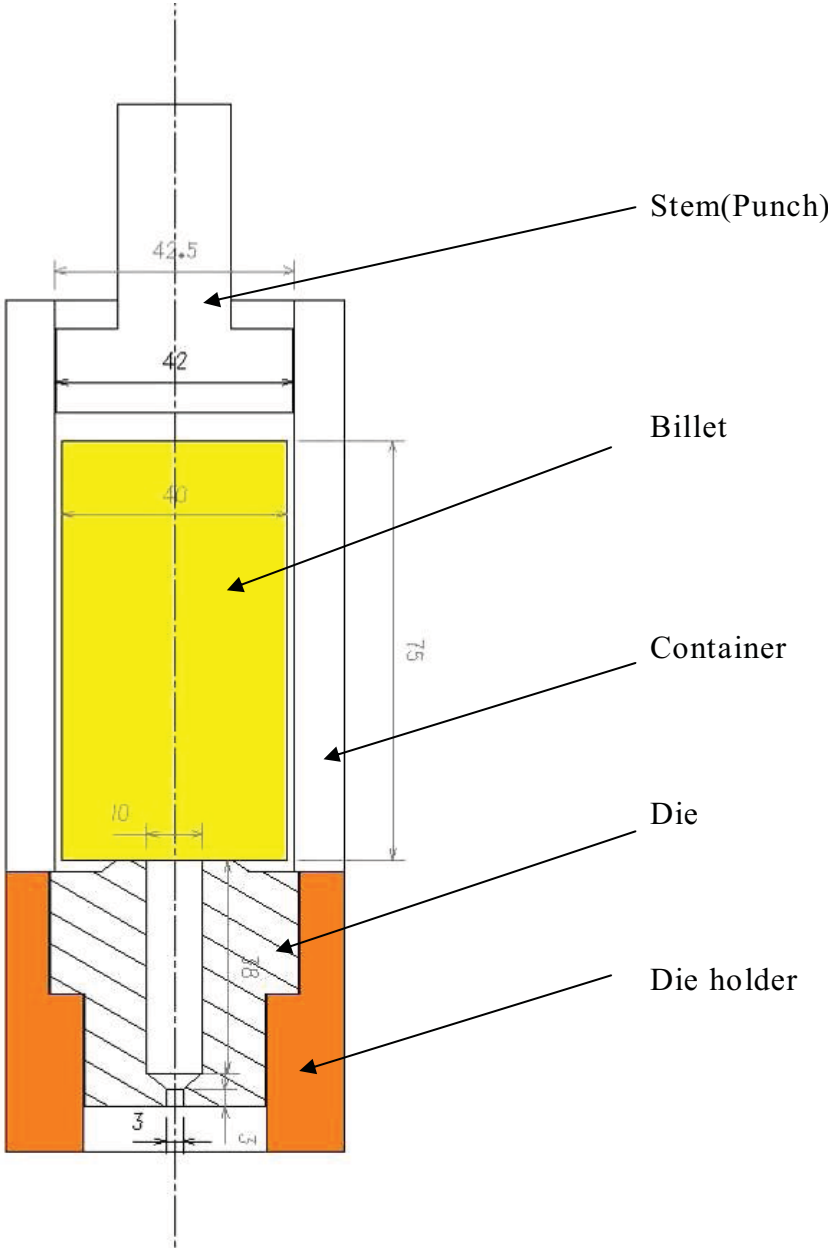
D$_0$=42.5mm: L=75 mm, d=40 mm D$_0$=42.5mm, d$_0$=42mm,   d$_1$=10mm,   d$_2$=3mm,
η=0.6, μ=0.32, L'=38mm,   , h$_0$=102mm, h$_1$=38mm,   h$_2$=3mm

Figure 26: The extrusion model of the test

5.4.2 Theoretical extrusion load calculation

Calculations of the loads and stresses that occur during extrusion are an important aid for production engineers in determining the ease with which a product can be extruded. For the toolmaker, press manufacturer and plant designer, this information helps in the design and layout of new plants. The extrusion load requirement of designed models should thus be calculated on a theoretical basis before the tests are made.

For direct extrusion, the total work W_T of extrusion includes W_S, W_{id} and W_F. Among them, W_F is the friction between the billet and the container. The ideal extrusion load F_{id} is obtained from the ideal work W_{id} of deformation. W_S is over and above the homogeneous work of deformation, to overcome the shearing deformation in the deformation zone.

The following expression can be obtained [26]:

$$F_T := F_S + F_{id} + F_F \tag{Eq.2}$$

The loads can be expressed as equation 3 and 4 [28]:

$$F_F := U \cdot L \cdot \mu \cdot k_f \tag{Eq.3}$$

$$(F_S + F_{id}) := A_0 \cdot \varphi \cdot k_w{}^! \tag{Eq.4}$$

Where U refers to the circumference of the container, L the instantaneous billet length and A_0 the cross sectional area of the container. The deformation resistance k_w differs from the flow stress, which is a material constant [26].

$$k_W := \frac{k_f}{\eta_F}$$

<div align="right">(Eq.5)</div>

In practice, the deformation efficiency factor of metal for example of aluminium is approximately 0.5 to 0.6 [15]. In this study, we take η with 0.6. Furthermore, the friction coefficient μ between steel and pure lead or lead alloy is approximately 0.32. The value is measured by a ring-compression-test, which was developed by Kunogi [29] . Plugging these values into Eq.5 results in a deformation resistance of lead at 53.3MPa at room temperature.

The total friction load was calculated in two phases during the extrusion process. Phase 1: extrusion of the billet from 40mm to 10mm in diameter. Phase 2: extrusion of the billet across the die land with an exit diameter of 3mm.

At room temperature, the flow stress of pure lead is 32MPa. Calculation using Eq.3 results in the following friction loads：

Phase1: $F_{F1} = \pi \cdot D_0 \cdot L \cdot \mu \cdot k_f = 3.14 \cdot 42.5 \cdot 75 \cdot 0.32 \cdot 32 = 102.5$ kN

Phase2: $F_{F2} = \pi \cdot d_1 \cdot L' \cdot \mu \cdot k_f = 3.14 \cdot 10 \cdot 38 \cdot 0.32 \cdot 32 = 12.3$ kN

Therefore, the total friction load of pure lead extrusion during the test process is calculated to be 114.8kN.

The compression load can also be calculated with Eq.4. The strain is related to the cross sectional area of container and extruded product.

$$\varphi := \ln\left(\frac{A_0}{A_1}\right)$$

<div align="right">(Eq.6)</div>

Calculating the cross section of container and extruded product from the diameter 42.5mm and 3mm and inserting the result into Eq.6 [12] leads to a strain $\varphi = 5.28$. Eq. 3 leads to the compression load of 389.77 kN. Therefore, the total extrusion load of pure lead during the process is calculated according to Eq.1 to be $F_T = 504.57$ kN.

Calculated the same way, the total extrusion load of lead-antimony alloy extrusion at room temperature is 1198.1 kN.

5.4.3 Test results and discussion

5.4.3.1 Quality of extrudes

Two spines were produced at room temperature through extrusion according to the method described in the previous section. Figure 27 shows the resulting lead and lead-antimony alloy extrudes.

It is notable that both spines have a good surface-quality without cracks, scratches or other defects. The final dimensions of these extrudes have a fairly good dimensional accuracy - within ±0.08 mm of the die dimensions.

Pure lead
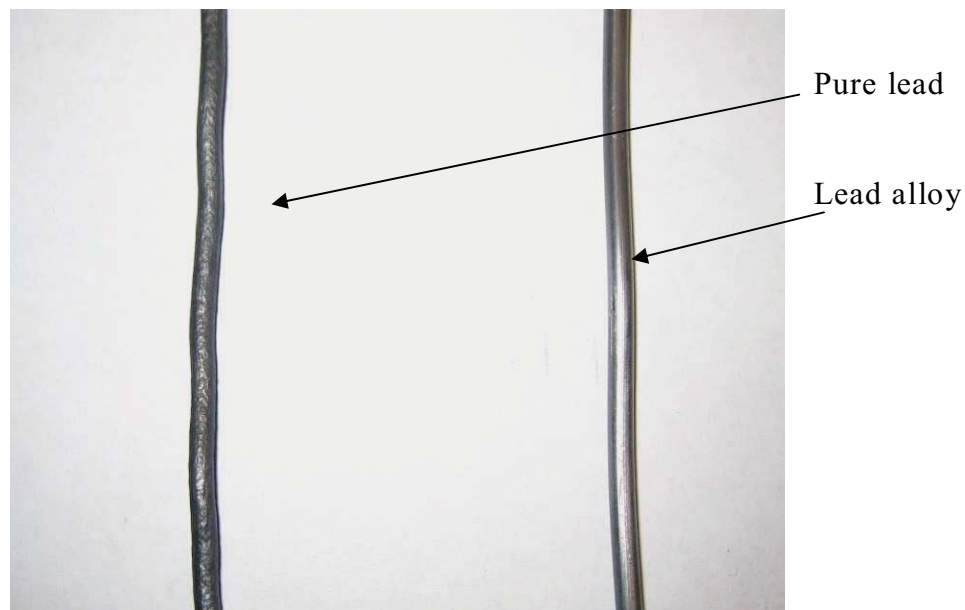
Lead alloy

Figure 27: Extrudes of pure lead and lead-antimony alloy with 3mm diameter

5.4.3.2 Extrusion load versus stem displacement curves

Figure 28a and 28b show the experimental results of extrusion load versus stem displacement observed during the extrusion of lead and lead alloy work pieces through the die.

The curves indicate two stages of extrusion, namely a sharp increase followed by a steady force. The area under the force-displacement curve represents the work. The increase in force is needed to initiate deformation. The maximum extrusion pressures for the various extrusion conditions are determined by dividing the maximum extrusion load by the original cross-sectional area of the work pieces.

Figure 28a and 28b indicate that the extrusion load for pure lead extrusion is 650kN, which is lower than the load for the extrusion of the lead alloy (820kN). This decrease in extrusion load for the specimen is due to the lower resistance to deformation offered by the metal as a result of its lower yield stress (flow stress) and lower hardening property.

Extrusion test of lead alloy(3.5% Sb)
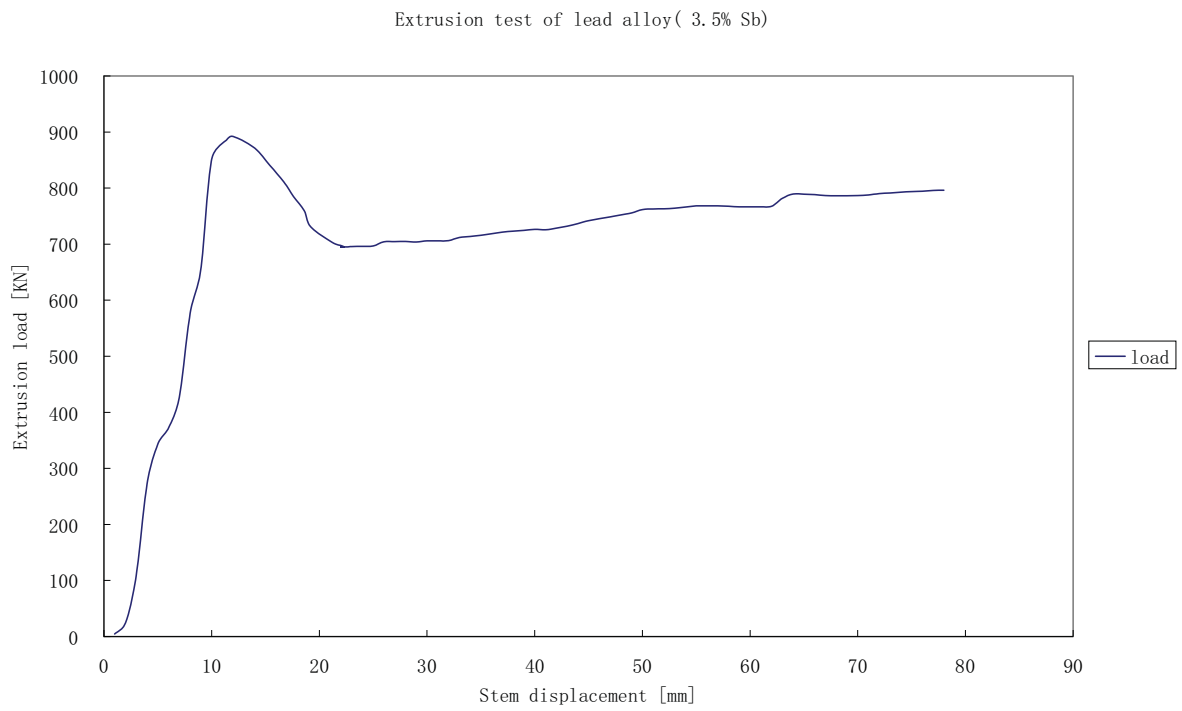
Figure 28 a: Extrusion load versus stem displacement of lead alloy

Extrusion test of pure lead
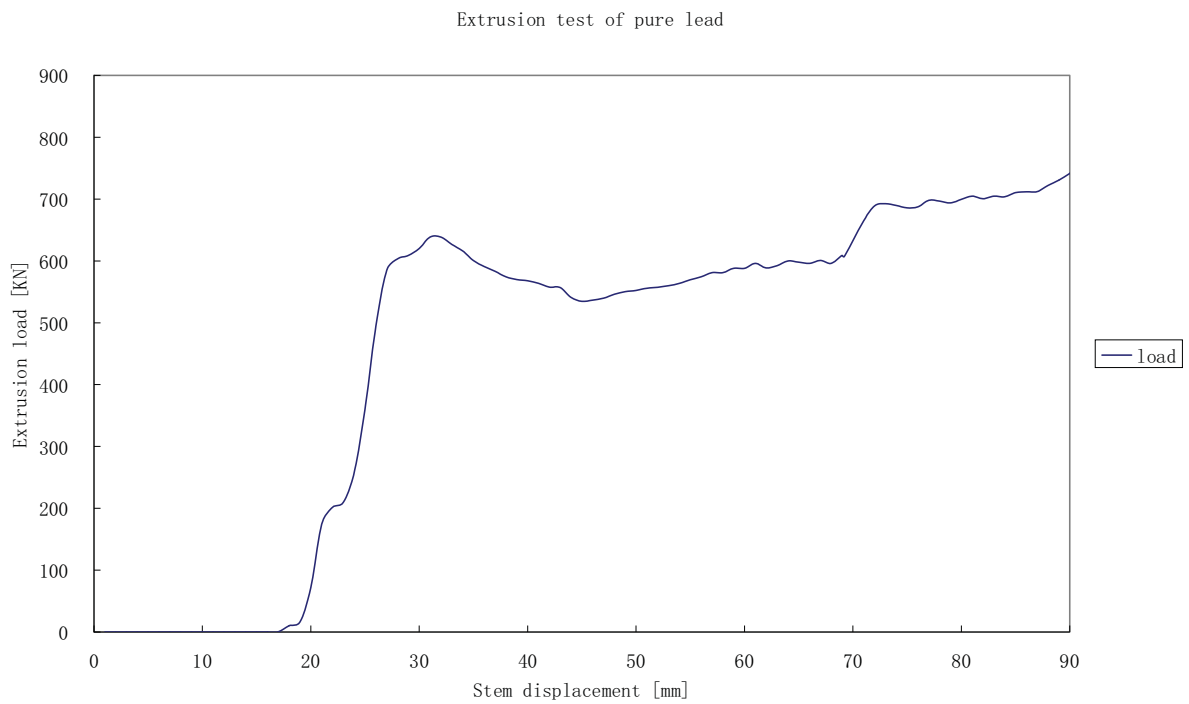
Figure 28 b: Extrusion load versus stem displacement of pure lead

The real extrusion loads of the test results were compared with the theoretical values calculated in 5.4.2. The deviations of true values are minimal: -0.28 for lead and +0.36 for the lead alloy.

5.4.3.3 Grain size of pure lead and antimony-lead alloy after extrusion test

Figure 29 a show the interior microstructure of the pure lead extrudes on a scale of 1:200µm. The picture indicates very course grains. In comparison, the grains of the lead-antimony alloy extrude are regular, thin and fine. No defects such as interior cracks, impurities or pores could be seen in either extrude.

The particular grain size and hardness of the extrude spines are recorded in Table 12. The grain sizes of the lead alloy became smaller after the extrusion, but the grain size of pure lead became larger.
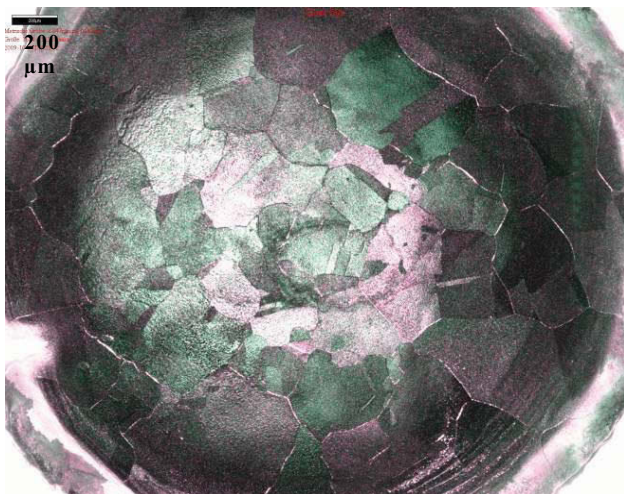
At the room temperature with φ=2,7   At the room temperature with φ=2,7
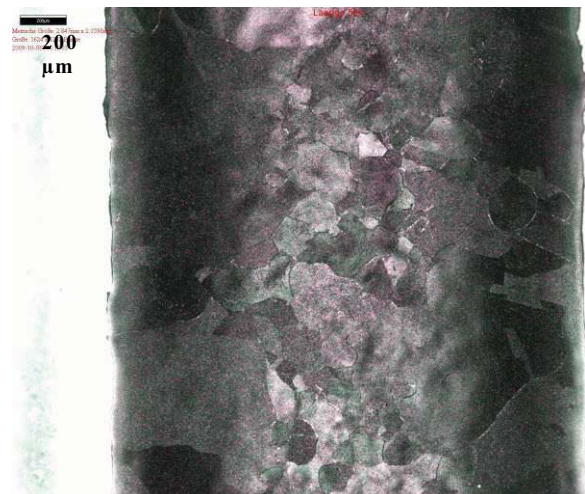
Cross section   Longitudinal section

Figure 29 a: Microstructure of pure lead extrude
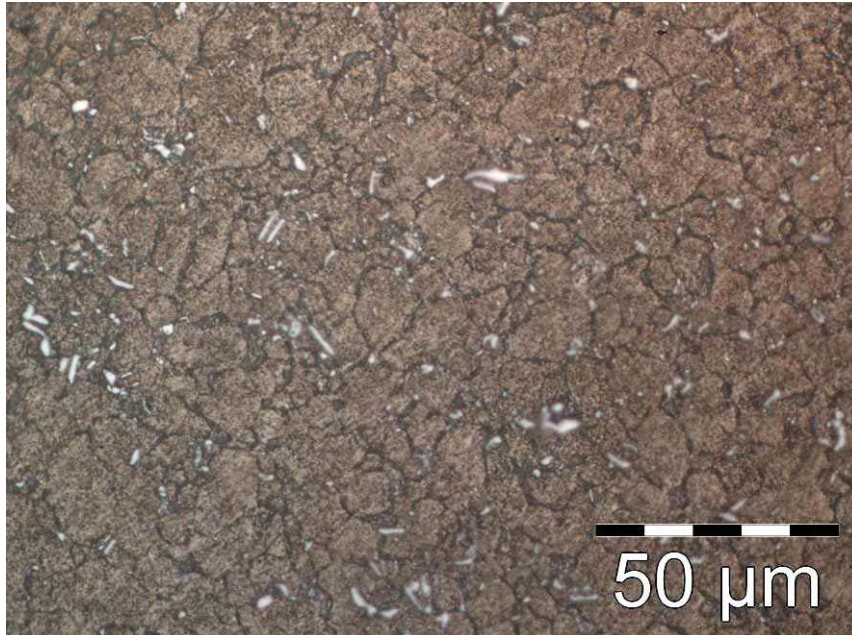
(i) At room temperature with φ=2.7, Cross section
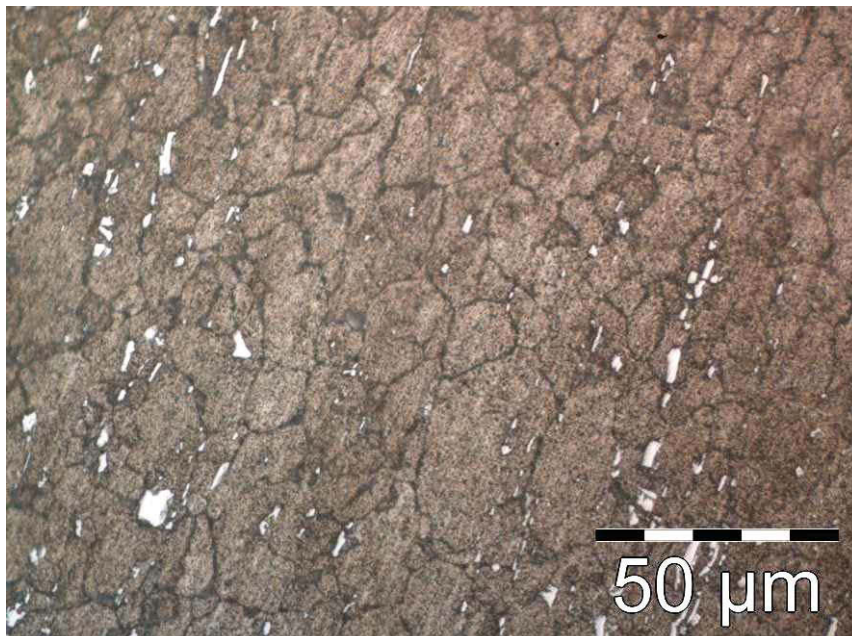
(ii) At room temperature with φ=2.7, Longitudinal section

Figure 27 b: Microstructure of the lead-antimony alloy (3.5% Sb) extrude

		ECD	**Elongation**	**Dmax**	**Dmin**
Pure lead	Cross section	227.15	1.79	340.05	310.31
	Longitudinal section	185.28	1.76	273.03	249.81
Lead alloy	Cross section	11.29	1.56	15.54	14.82
	Longitudinal section	11.50	1.81	17.11	15.97

Table 12: Grain parameters of the pure lead and lead-antimony alloy after extrusion

ECD: Equivalent circle diameter

Dmax: average maximum grain size

Dmin: average minimum grain size

5.5 Influence of oxide films on metal lead surface by compression

5.5.1 Compression test of lead blocks with oxide films.

In order to investigate the effect of an oxide film on the surface of lead during production, the following experiment was made. Two pieces were cut off a lead ingot. As lead oxidizes easily when exposed to oxygen, an oxide film covers the surfaces of the two lead blocks. A load was used to compress the two blocks together as shown in Figure 30 a. The surface in contact with each other were not treated and chosen randomly.

(a) The two blocks are compressed together

(b) After compression

Schliffbilder

(c) Cross section of the compressed block

Figure 30: Compression test of two lead blocks

5.5.2 Test results and discussion

Compression had an effect similar to cold-welding. Because the contact surfaces are relatively smooth, the Van der Waals forces are able to draw the two pieces together

and even eliminate the macroscopic interface. Figure 31 shows the macrostructure of the cross section of compressed block. The continuous horizontal line pictured represents where the two surfaces (oxide layer) met. No gap remains between the two lead blocks after compression.
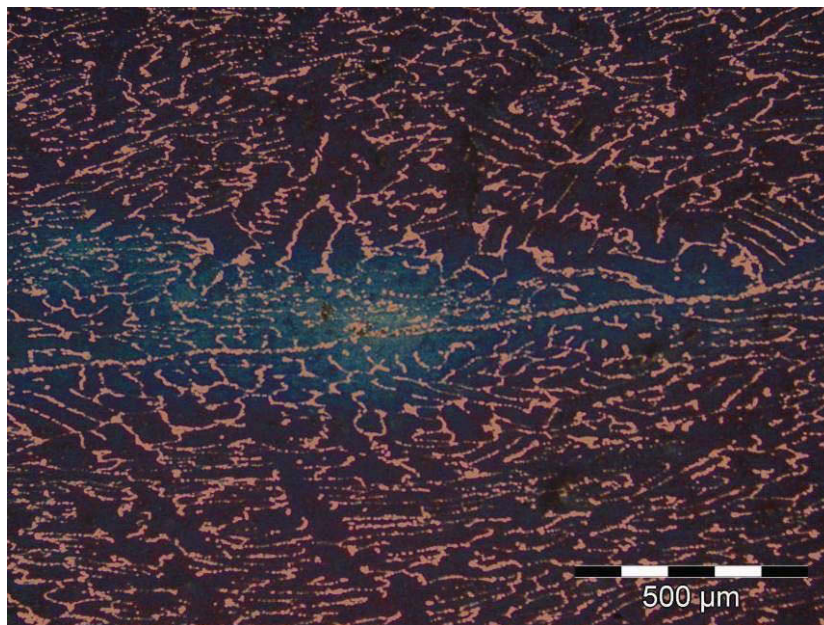
Figure 31: Macrostructure compressed block

The results of this experiment lead to the conclusion that material could be saved in the case of an industrial application. The remaining material from one extrusion may be combined with new material for a second extrusion (billet-to-billet extrusion). Furthermore, a surface treatment for removing the oxide layer is not necessary.

5.6 Extrusion of tubular plate in laboratory

Based on the data and results of the previous experiments, an appropriate extrusion-die was designed. Using this tooling, a lead-electrode plate was manufactured directly by extrusion forming including shutters and spines.

Note that this experiment was only conducted using the lead-antimony alloy. The reasons for this are:

1) The lead alloy has a better conductivity and hardness than pure lead,

2) As discovered in previous experiments, the grain refinement effect of lead alloy is significantly better than that of pure lead after extrusion.

5.6.1 Design of the extrusion model

Depend on the geometry of the plate; the extrusion model should be relevantly designed. The die is made up of two pieces, and they are symmetrically fixed with each other by bolt or clamp. The advantage of this design is in order to make the plate take out more easily from the die after extrusion. The die should also be grooved with 5-6 mm deep and 80 mm wide. Five apertures with 8mm diameter are drilled in the bottom of this groove. The raw material can be pressed into designed figure through these apertures during the extrusion test. That also means that the function and structure of the die and container are integrated. The following picture shows the specific structure of the extrusion die.
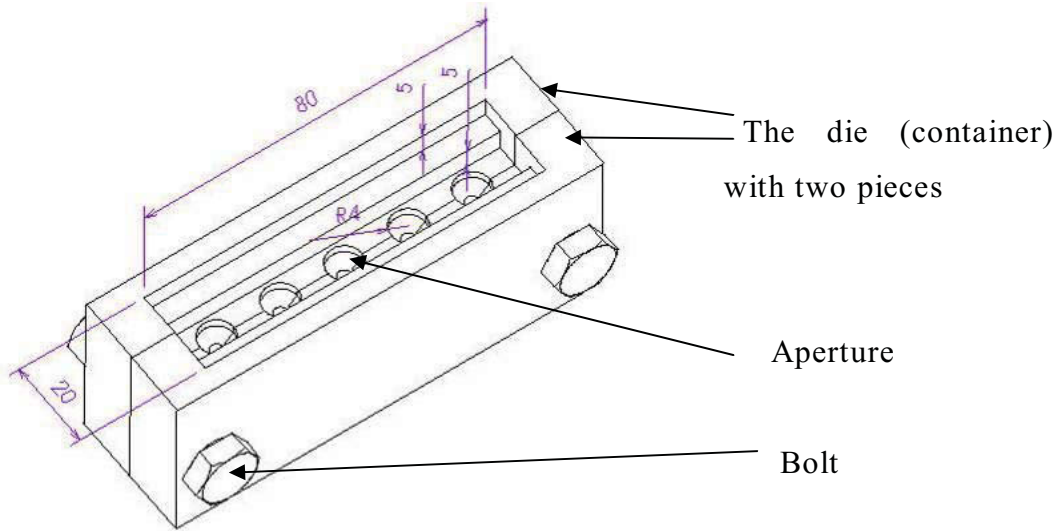
Figure 32: Extrusion die made in the laboratory

5.6.2 The theoretical extrusion load in multi-hole extrusion

Bars and simple shapes are extruded through multi-hole dies to increases productivity. The number of die apertures that can be used increases with smaller and simpler sections. For a constant billet diameter, the extrusion ratio reduces as the number of strands n is increased. Consequently, the extrusion load decreases linearly with the natural logarithm of extrusion ratio, according to the relationship [26]:

$$F_{id} := A_0 \cdot k_w \cdot \ln\left(\frac{A_0}{n \cdot A_1}\right) \qquad (\text{ Eq. 8 })$$

In this case, the diameters of the multi-hole die are showed in the Figure 32 and Figure.34. The cross sectional area of the container A_0 is 640 mm^2 which is the product of the form length l=80mm and width b=8mm. The cross sectional area of the extrude produced is the sum of the area of five extruded spines which is equal to 35.325 mm^2. The logarithmic strain of extrusion is be calculated according to Eq.8 to be $\varphi = 2.9$. Finally, F_{id} is calculated to be 235 kN.

F_{id} represents the ideal extrusion load. The total load is also relevant to the F_F or friction load. According to Eq.8, the sum of friction load between billet/container and billet/die does not exceed 50 kN, hence the total extrusion load is approximately 290 kN.
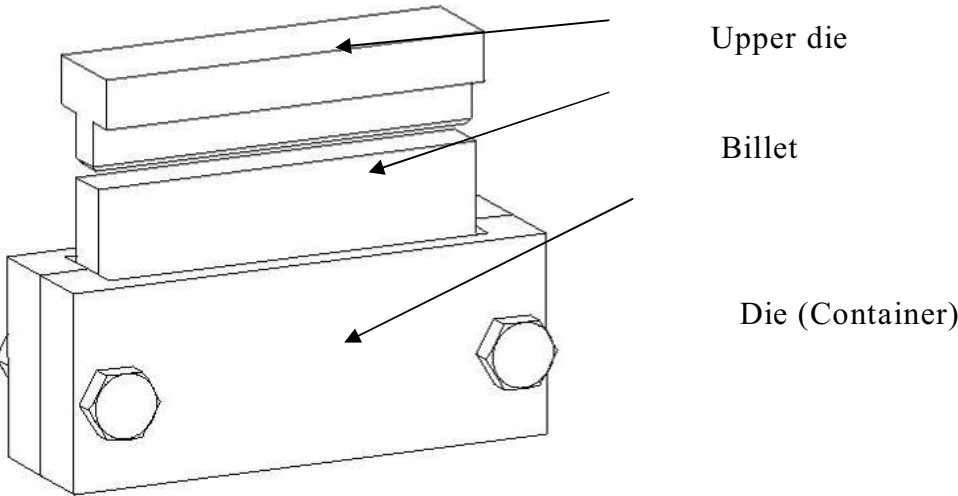
Figure 33: Multi-hole extrusion model
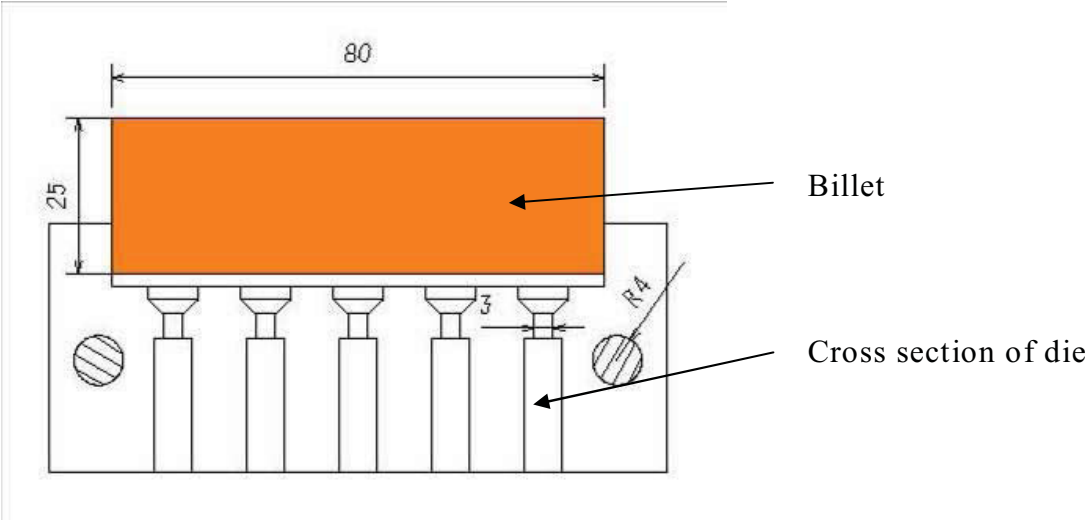
Figure 34: The cross section of the extrusion die

5.6.3 Test results and discussion

5.6.3.1 Quality of the extruded product

A small tubular plate in which five spines are connected by a top bar was extruded using the die described above. Figure 35 shows the extruded plate.

Figure 35: Tubular plate with five spines extruded in the laboratory

The extruded tubular plate was investigated for quality characteristics such as dimensional accuracy, product curvature and piping defects.

The dimensional accuracy of tubular plates was checked, using a vernier caliper to compare the dimensions of the tubular plate with the dimension of the dies. The diameter of the spine was measured to be 3mm±0.2mm. The surface of tubular plate is smooth without cracks, scratches or other visual defects. The connection and transition between the spines and top bar is acceptable, proving that the material flows well in the extrusion-die during the test.

Figure 36 shows the detail of longitudinal section of the plate. The grains are also fine and uniform.

Figure 36: Longitudinal section of the plate

5.6.3.2 Multi-hole extrusion load versus stem displacement curve

During the extrusion test, the extrusion load versus stem displacement was recorded. The resulting curve is pictured in Figure 37. Note that the bolts in the die broke after plastically deforming during the course of the experiment, ultimately influencing the curve. A curve similar to that in 5.4.3 was expected.

As the diagram shows, the force increases with increasing stem displacement during the extrusion process. The maximal value of force reached during the test is 400kN, whereas the theoretical total load calculated as the sum of extrusion and friction load was 290kN. The difference may be explained by the error involved in calculating the

friction force between die land and billet. In practice, the battery plate would be larger than the sample extruded in the laboratory; therefore an even greater force would be required.
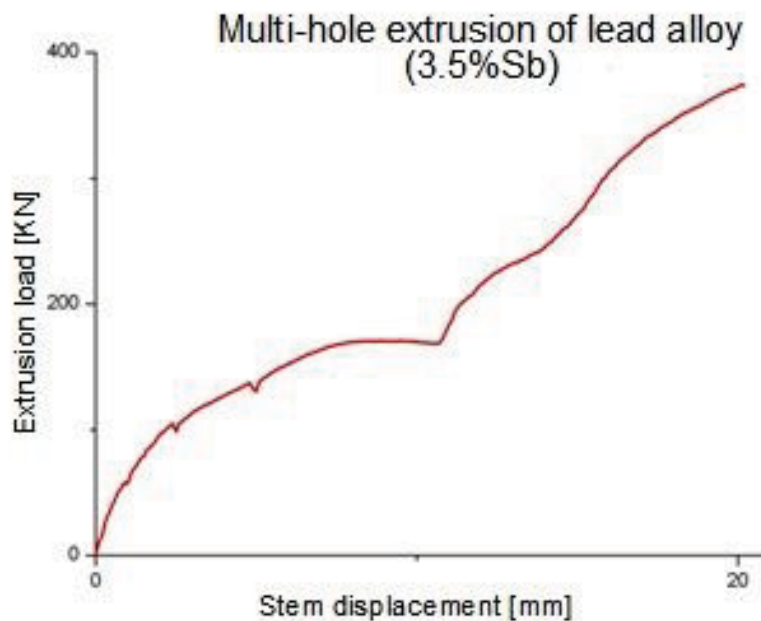
Figure 37: Extrusion load versus stem displacement during multi-hole extrusion

5.6.3.3 Discussion

This experiment resulted in a tubular plate of good quality and the required force of extrusion was much less compared to that of other metals. Therefore, an industrial application for tubular plate production according to this method is proposed. As the standard tubular plate consists of 19 spines, the die geometry and process parameters must be designed accordingly. In addition, improvements can be made to influence the surface, quality and geometry of the tubular plate.

6 Discussion, conclusion and future prospects

6.1 Comparison of different manufacturing methods

As mentioned in the beginning chapters, the most conventional method of battery-plate production is casting and the disadvantages were analysed. Cold forming on the other hand has several advantages for industrial production:

➢ No oxidation or gas\metal reactions.

➢ Higher mechanical properties are obtained by cold working

➢ Narrow tolerances

➢ Better surface finish

➢ Grain size is much finer and thinner than castings

➢ No poison vapor

Consequently, the conclusion can be drawn that cold extrusion forming is a more ideal method for battery-plate production. However, there are also different methods of cold forming. Various methods will be described in the following section.

1. One-piece extrusion forming.

We can use one-piece extrusion forming method to manufacture a tubular plate, similar to that previously manufactured in the laboratory. The die will be designed according the dimensions required of the battery electrode plate. This method offers several advantages. No additional processing is required, such as cutting away excess stocks or connecting spines to carrots and the top bar. The finished product has a very good geometric precision.

2. Multi-piece extrusion forming.

Taking in account the requirement of raising productivity, a multi-piece extrusion forming method could be used to manufacture the tubular plate, as shown in Figure 37. The raw material is extruded as a particular form similar to a heat sink. After extrusion, the work piece is cut to obtain single plates.

There are disadvantages to this method. There are dimensional differences between the ideal top bar of a tubular plate and the final product which is obtained by cutting the extrude work piece. That means the top bars require re-processing after cutting.
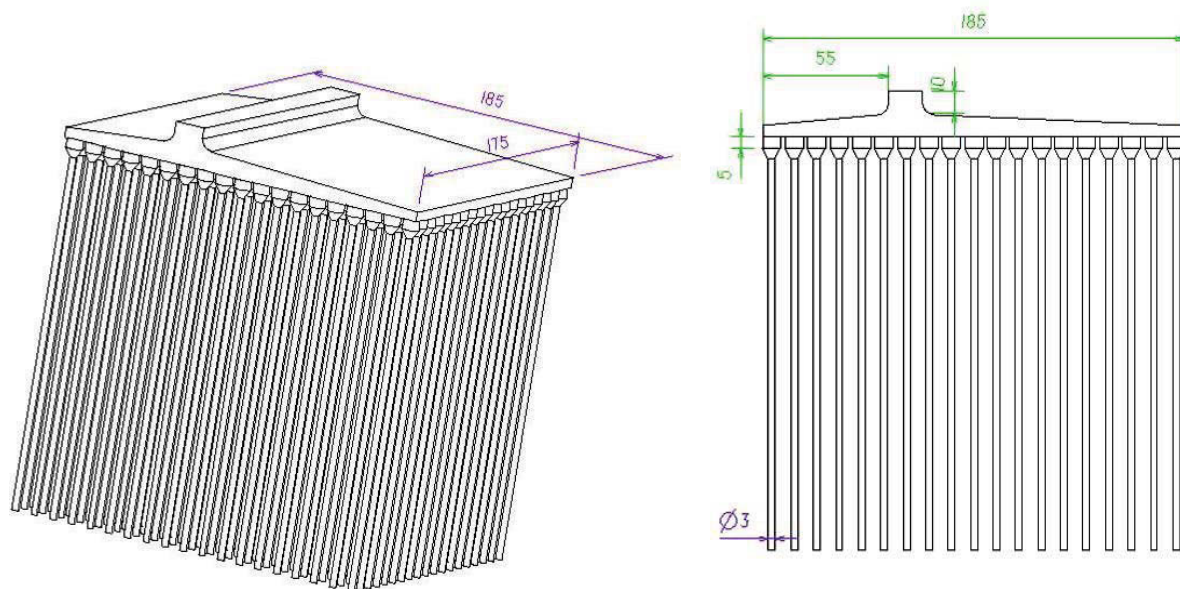
Figure 38: The multi-piece extruded work piece

3. Single extruded spines connected to the carrot and top bar

The spines are extruded and the top bars and carrots are manufactured by casting or forming. The remaining issues are the connection of the spines, carrots to the top bars. Figure 38 a and 38 b show they can be connected via cold welding or induction welding methods. However, surface treatments are required before welding. Furthermore, the oxide layers, which exist between the connecting surfaces, may cause a decrease in the electrode conductivity of the electrode plate.
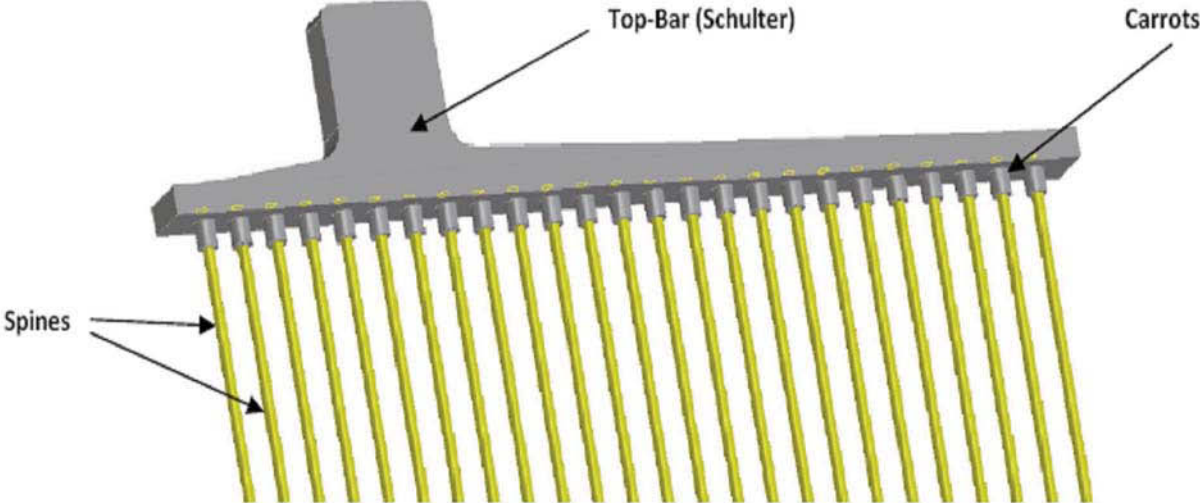
(a) The connection of spines, carrots and one piece top bar through induction welding
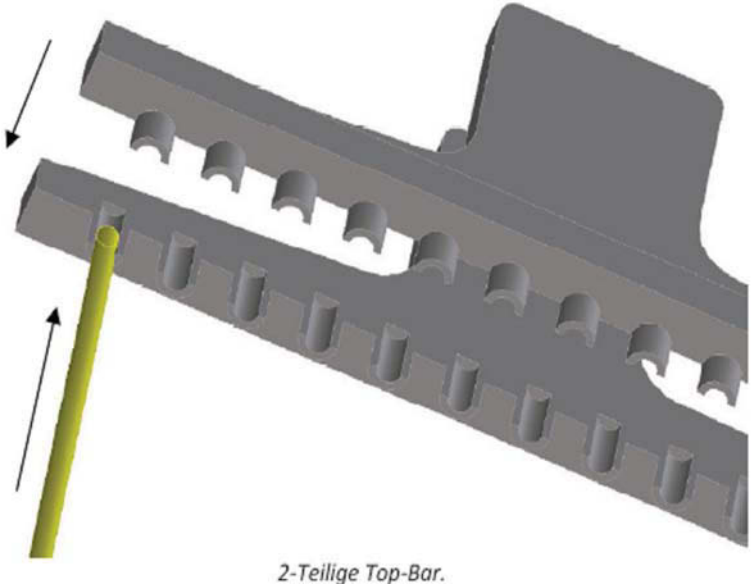
(b) The spines are pressed between two top halves.

Figure 39: Possible connections between top bar and spines

6.2 Process layout for industrial production

One-piece and multi-piece extrusion is relatively good methods. In industrial production, not only the quality and cost of the product are important, but also the control over and operation of the process should be manageable. For this reason the follow approaches should be considered in the design of the process layout:

➢   Design of the extrusion-die and its upper

The design of the extrusion-die and its upper depends on the geometrical product requirements. For example, the quantity of spines in a tubular plate, the dimensions of the top bars, thickness of carrots connecting the spines to the top bar and the chamfer at the transition section.

➢   Calculation and simulation

The forming process can be simulated to calculate important parameters before production is implemented. For example, the load requirements, the weight or volume of raw materials for a single extrusion process, even the dead metal zone of the work piece during extrusion is visible in a simulation. At the same time, the design of die and its upper can also be improved according to the results of the simulation.

➢   Preparation of material

The raw materials should be cut to fixed geometries that suit the size of the die and container.

➢   Extrusion and deforming

The raw materials are extruded with designed die model. The work piece is taken out of the die when the extrusion process is completed. Excess stocks of the plate inconsistent with production requirement should be cut off. For example, spines with different lengths should be cut to be equal in length.

6.3 Conclusion and future prospects

Lead and its alloys have very good ductility. In general, the compression or extrusion temperatures have a strong influence on the flow stress. But experimental results show that the flow stress of lead and its alloy are 30MPa and 76MPa respectively at room temperature. That means that the forming load required during the forming process is not so large.

Compared to the casted condition, the extruded alloys posses much finer grain size and consequently much better mechanical properties. The micrographs of extrudes show there are no internal defects such as holes, porous, inclusions or cracks. The density of materials is increased after extrusion. A further advantage is that spines with finer grains can absorb active materials better than those with coarser grains.
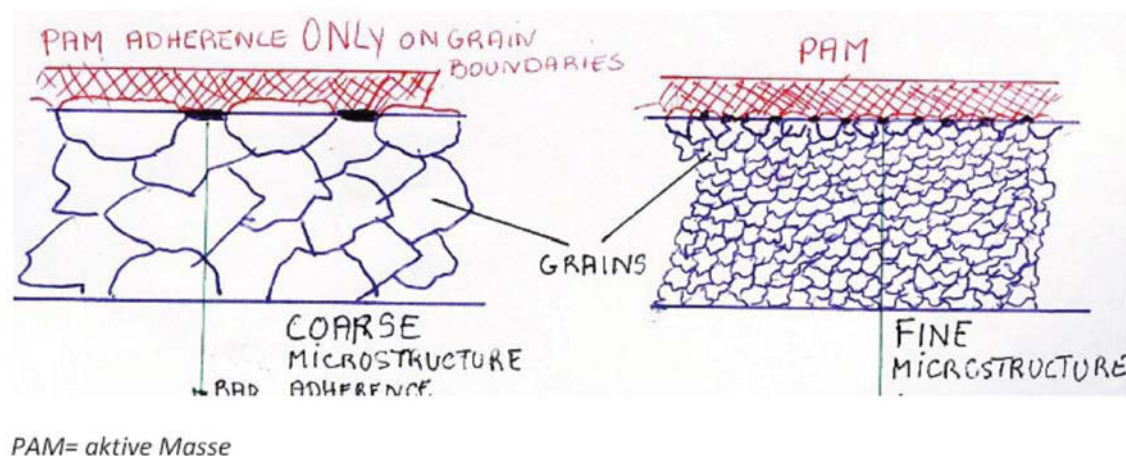
Figure 40: Material adsorption of grains

The tubular plate manufactured by the cold forming process has excellent geometrical accuracy. The spine of the sample tubular plate made in the laboratory was within a tolerance of ± 0.21mm of the extrusion die. There were no cracks or

deformation due to heat shrinkage in the extruded tubular plate as the process was not hot.

Of the various extrusion molding methods discussed, the multi-piece extrusion molding method is the most efficient for industrial applications as the connection problem between the spines and top bar are avoided. Therefore, further steps in the process are also avoidable.

In conclusion, forming (extrusion) at room temperature for tubular plate manufacturing is not only economical and environmentally friendly but also very effective. The results of the series of experiments performed confirm that tubular plate extrusion at room temperature is practical.

For future industrial production, it would even be possible to use a different die to change the cross section of the extruded tubular plate spines for the sake of reducing the amount of raw material used and cutting costs. The spines may even be extruded together with a core out of a more conductive metal, which could improve the product quality.

7 References

[1] Cowlishaw, M. F., *The Characteristics and use of lead-Acid Cap Lamps*, Trans. British Cave Research Association, Vol 1, No. 4, December 1974, pp199-214.

[2] *Primer on lead-acid storage batteries,* US Department of Energy, DOE-HDBK-1084-95, Washington D.C., 205585, September, 1995.

[3] Saupe, Gerhard, *Photovoltaische Stromversorgungsanlagen mit Bleibatteriespeichern: Analyse der Grundprobleme, Verbesserung der Analgentechnik Entwicklung eines Simulationsmodells fuer Batterie*, Thesis of Universitaet Stuttgart, OCLC: 75446277, 1993.

[4] *Bestimmungen fuer Akkumulatoren und Akkumulatoren-anlage,* DIN VDE-Norm 0510/60, 1977.

[5] BM-Battery Machines, www.bm-batterymachines.com, December 2009.

[6] www.en.wikipedia.org/wiki/lead-acid_battery.

[7] Lead Battery Manufacturing, U. S. Department of Labor, www.osha.gov/SLTC/etools/battery_manufacturing/index.html.

[8] www.varta-automotive.com

[9] *Battery design flat plate versus tubular*, www.bulldog-battery.com

[10] www.jgdarden.com/batteryfaq

[11] Degarmo, E. Paul, Black J. T., Kohser, Ronald A., *Materials and processes in manufacturing*, 9th ed., Wiley, ISBN 0-471-65653-4, 2003.

[12] Schleg, Frederick P, Kohloff, Frederick H., Sylvia, J. Gerin, *Technology of metalcasting*, American Foundry Society, 2003.

[13] Drotschmann. C., *Bleiakkumulatoren*, Verlag Chemie,Weinheim, 1951, pp. 132-145

[14] M. Bauser, G. Sauer, K. Siegert, *Strangpressen*, Aluminium Verlag GmbH, Duesseldorf , 2001.

[15] K. Laue, H. Stenger, *Extrusion: Processes, Machinery, Tooling*, 5th ed., ASM, Ohio, 1981, ISBN: 0871700948.

[16] Charles Wick, Raymond F., Veilleux, *Tool and manufacturing engineers handbook: Forming,* Society of Manufacturing Engineers (SME), 1949, ISBN: 0872631354

[17] Amann, Erwin, *Einfuehrung in die Grundlagen der Umformtechnik*, Prost & Meiner verlag, Coburg, 1966.

[18] D.R.Blaskett, D.Boxall, *Lead and its all*oys, Ellis Horwood, New York, 1990, ISBN: 0135286964.

[19] Wilhelm Hofmann, *Lead and lead alloys Properties and Technology*, Springer-Verlag, Berlin, 1970.

[20] W.T. Read, *Dislocations in crystals*, McGraw-Hill, New York, 1953.

[21] Sivaraman Guruswamy, *Engineering properties and applications of lead alloys,* International Lead Zinc Research Organization, New York, 2000.

[22] R. S. Dean, *The Lead-Antimony System and Hardening of Lead Alloys,* AIME Transactions, Volumen 73, 1926, pp. 505-529.

[23] I. Karakaya, W.T. Thompso, *The Pb-Sn System*, Journal of phase equilibria, New York, ISSN 1054-9714, Volume 9, Number 2, 2008.

[24] V. Loebe, *Metallurgie 8*, Einschließlich der Elektrometallurgie, Forschritte Chemie, 1911, pp 255-276.

[25] K. Osamura, *The Pb-Sb-Sn system*, Jouranl of phase equilibria, New York, ISSN: 1054-9714, Volume 6, Number 4, 2008.

[26] H.Stenger, K. Laue, *Extrusion--Processes, Machinery, Tooling*, American Society for Metals, Metals Park, Ohio, 1981.

[27] W.W. Krysko, M.W.Lui, *Untersuchungen ueber das Strangpressen kuebisch-flaechenyentrierter Metalle Teil II: Kraftbedarf und Kraftverteilung ,* Materialwissenshaft und Werkstofftechnik, Volume1 Issue 2, Weinheim, September 2004.

[28] E. Siebel, E. Fangmeier, *Untersuchungen ueber den Kraftbedarf beim Pressen und Lochen*, Mitt. Kaiser-Wilhelm Inst., Eisenforschung 13, Duesseldorf, 1931.

[29] M. Kunogi, *On plastic deformation of hollow cylinder and axial compression,* Journal of the Scientific Research Institute, 1954, pp. 63-92,.

[30] Robert E. Reed-Hill, Reza Abbaschian, Lara Abbaschian, *Physical metallurgy principles, Edition: 3rd ed.,* Cengage Learning, Stamford, 1970, ISBN: 9780495082545

[31] *Battery paste dispersant.* US Patent 5948567, September 7. 1999.

[32] *Tech Notes: Properties of lead,* Advanced Materials & Processes, Volume 166, Issue 9, September 2008.

[33] David Linden, Thomas B. Reddy, *Handbook of batteries*, McGraw-Hill, New York, 2002, ISBN: 0071359788.

[34] *ToxFAQs: CABS^{TM}/Chemical agent briefing sheet, lead,* Agency for Toxic Substances and Disease Registry/Division of Toxicology and Environmental Medicine, 2006.

[35] Mari S., Golub, *Metals, fertility, and reproductive toxicity*, Taylor & Francis Group, 2006.

[36] Pearson C.E., Parkins R.N., *The extrusion of metals*, John Wiley, London, 1944.

List of Figures

List of Tables